PREPARATION OF ORGANIC POLYMER-SILICA NANOCOMPOSITES AND STUDY OF THEIR ADSORPTION CHARACTERISTICS

BY
MOHAMMAD ABU YOUSUF

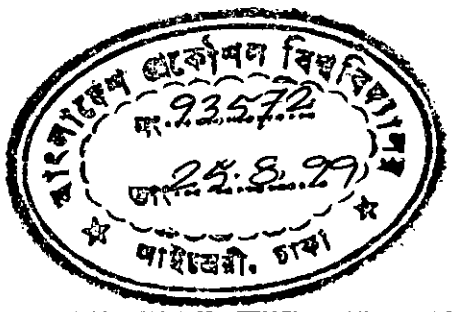

SUBMITTED IN PARTIAL FULFILMENT OF THE REQUIREMENTS FOR THE DEGREE OF M. PHIL IN CHEMISTRY

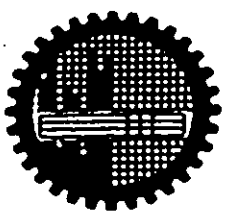

DEPARTMENT OF CHEMISTRY
BANGLADESH UNIVERSITY OF ENGINEERING AND TECHNOLOGY
DHAKA-1000, BANGLADESH
AUGUST-1999

Dedicated
To
My beloved Parents

DECLARATION

This thesis work has been done by the candidate himself and does not contain any material extracted from elsewhere or from a work published by anybody else. The work for this thesis has not been presented elsewhere by the author for any degree or diploma.

Mohammad Abu Yousuf
(Candidate)
M.Phil Student
Roll No. 9503009
Session: 1994-95-96
Department of Chemistry
BUET, Dhaka
Bangladesh

CERTIFICATE

This is to certify that the research work embodying in this thesis has been carried out under my supervision. The work presented herein is original. This thesis has not been submitted elsewhere for the award of any other degree or diploma in any University.

Dr. Al-Nakib Chowdhury
(Supervisor)
Assistant Professor
Department of Chemistry
BUET, Dhaka
Bangladesh

Bangladesh University of Engineering and Technology, Dhaka
Department of Chemistry

Certification of Thesis

A thesis on

"Preparation of organic polymer-silica nanocomposites and study of their adsorption characteristics"

By

Mohammad Abu Yousuf

has been accepted as satisfactory in partial fulfilment of the requirements for the degree of Master of Philosophy (M. Phil) in Chemistry and certify that the student has demonstrated a satisfactory knowledge of the field covered by this thesis in an oral examination held on August 14, 1999.

Board of Examiners

1. Dr. Al-Nakib Chowdhury
   Assistant Professor
   Department of Chemistry
   BUET, Dhaka
   — Supervisor & Chairman

2. Dr. M. Muhibur Rahman
   Professor, Department of Chemistry
   University of Dhaka
   — Co-supervisor

3. Professor Dr. Enamul Huq
   Head, Department of Chemistry
   BUET, Dhaka
   — Member (Ex-officio)

4. Dr. Md. Monimul Huque
   Professor, Department of Chemistry
   BUET, Dhaka
   — Member

5. Dr. Abu Jafar Mahmood
   Professor, Department of Chemistry
   University of Dhaka
   — Member (External)

Acknowledgement

I am extremely indebted to my respected supervisor Dr. Al-Nakib Chowdhury, Ph. D. (Japan), Assistant Professor, Department of Chemistry, Bangladesh University of Engineering and Technology (BUET), Dhaka, Bangladesh, for his careful guidance through out the period of this dissertation. I could not thank him enough for his timely suggestion and through scrutiny, carefully reading of my work and the countless hours of discussion that were invaluable at every stages of this study.

I express sincere gratitude to my reverend teacher Professor M. Muhibur Rahman, M. Sc. (Dhaka), Ph. D. (Cambridge), Department of Chemistry, University of Dhaka, for his scholastic supervision, erudite discussion, invaluable suggestion and constructive guidance throughout the progress of this research work without which the present achievement would have not been materialized.

I am obliged to Professor Dr. Enamul Huq, Head, Department of Chemistry, BUET, for his hearty co-operation and inspiration during this research. I am highly grateful to Professor Dr. Monimul Huque, Professor Dr. Manwarul Islam, Mr. Md. Nurul Islam and Professor Dr. Motiur Rahman, Department of Chemistry, BUET, for their constant supports and suggestions throughout the work. I am also grateful to all other teachers and staff of Chemistry Department, BUET, Dhaka.

I, want to thank Dr. Md. Aminur Rahman, Ph. D. (Japan), SSO, IGCRT. BCSIR, Dhaka for his help in the present research works. I also thank to Arifur Rahman, Ruhul Amin Khan, M. Quamrul Hasan, Akhtar Hossain, Shakhawat Hossain and Rabbani for their constant help.

I wish to render my thanks to all my friends and colleagues including Harun-Or-Rashid, Ahsan Habib, Tarit, Abdullah, Tyebur Rahman, Arif Hossain and Abul Kalam Azad. Special thanks to Mrs. Nurtaj Begum for her sincere help and sacrifice during the present work.

I am highly grateful to the authority of BUET and BIT-Khulna for giving the opportunity of research and the financial support for the work.

Last but not least, the co-operation and encouragement of my parents, elder brother, Mr. Mahabubur Rahman Chowdhury and Mrs. Helena Begum and Moni, inspired me to work long and often frustrating hours, but always keep in good sprit.

Special thanks to Mr. Md. Fakhruzzaman for computer composing and printing of this thesis.

Mohammad Abu Yousuf

Author

CONTENTS

Abstract

Polymerization of aniline, *o*-toluidine and 2-chloroaniline from an aqueous solution containing sodium silicate yielded stable poly(aniline)/silica, poly(*o*-toluidine)/silica and poly(2-chloroaniline)/silica composites. Synthesis was carried out at different pH, viz. 3.1, 7.0 and 11.3 and at different temperatures, viz. 0^0C, 27^0C and 50^0C and stable poly(aniline)/silica, poly(*o*-toluidine)/silica and poly(2-chloroaniline)/silica nanocomposites was found to be formed in the reaction mixture under the experimental conditions employed. These composites have been characterized in their solid states by a wide range of experimental techniques including optical microscopy, infra-red spectroscopy and sedimentometry for particle sizing. Adsorption studies with these composites employed inverse gas chromatography and BET surface area measurement.

Elemental analysis for the silica content of the composites was performed by well known hydrofluorization method and silica content up to 11% in the matrix was obtained. Density of the bulk polymer and the polymer/silica samples were measured by micromeritics multivolume auto pycnometer and clearly different density values were obtained for the samples. The particle size distribution of the composites observed with sedigraph shows that the particle diameter varies from 40-1 μm. However particle size below 1 μm could not be detected due to the limitation of the micromeritics instrument. A wide distribution of white images in the micrographs of polymer/silica samples was observed and this may be attributed to the presence of silica particles in the composite matrix.

Infra-red spectroscopic studies yielded qualitative information on the polymer/silica composites. In the spectra, the characteristic bands of aniline, *o*-toluidine and 2-chloroaniline were observed which confirmed the presence of these monomer rings in the respective polymer. The infra-red spectra observed for the studied samples exhibited absorption bands attributable to both the polymer and the silica components.

Characterization of poly(aniline) and polymer/silica nanocomposites by inverse gas chromatographic technique was performed. For this purpose, composite materials were used as fine column material. These composite materials when packed in the IGC column were found to be capable of separating a mixture of alkanes (C_5-C_9) indicating that these composites can be used as column materials. IGC measurements also indicated higher surface energy values of the composite materials than that of the bulk polymer.

BET technique was employed to measure surface area of the bulk poly(aniline) and the polymer/silica composites. In order to evaluate the surface area of the matrix the adsorption isotherms were fitted to the BET equation. Surface area was evaluated for all the studied samples from the linear plots of the adsorption data according to the BET equation. Experimentally observed surface area of the bulk polymer was much smaller than that of the corresponding polymer/ silica matrices. Change in the synthesis conditions e.g., pH and temperature, yielded products with different surface areas although all the samples contain almost the same amount of silica. This finding indicates that the synthesized materials may differ in porosity and particle size to exhibit different surface area of the studied samples which were prepared under different synthesis conditions. However, BET measurements with poly(*o*-toluidine)/silica and poly(2-chloroaniline)/silica indicated relatively smaller surface area than the

other composites investigated and may be due to the presence of bulky $-CH_3$ and –Cl groups in the polymer backbone. These bulky moieties may hinder the accumulation of appreciable amount of nanoparticles into the sample framework and consequently results in a relatively lower surface area.

Chapter 1
Introduction

1.1 Brief history of the composite materials

Composite materials involve some combination of two or more components from the 'fundamental' materials. A key philosophy in selecting composite material is that they provide the "best of both worlds", that is, attractive properties from each component.

Composites have acquired a leading position in the development of new materials because of the realization that with judicious choice of combinations of materials startling new combinations of properties can be obtained.

In the past three decades, light weight, corrosion resistant, high performance composite materials have increasingly been used to replace conventional materials used in the construction of space vehicles, military and civilian aircraft, rockets, boats, ships, buses, trucks, automobiles etc. Upto 15% weight reduction in planes has been achieved by using composite materials in place of metals thereby leading a to a higher payload.

The development of these high performance composites has been possible due to the availability of high strength, high modulus fiber as reinforcement and organic matrix resins capable of sustaining high loads and stresses over a prolonged period of time and wide temperature range.

Epoxy resins are the most widely used polymer matrix materials because of their excellent mechanical properties and processing characteristics. However advanced composite structures exposed to high temperatures (>150^{0}C) have to be fabricated from resins matrices having thermal/moisture resistance better than the state-of-the-art epoxy resins. In order to meet these requirements a family of addition polyimides having vinylic or acetylenic unsaturation have been developed in the past. Rismaleimide and endo-5-norbornene-2, 3-

dicarboximide endcapped imide resins have been investigated as matrix resins for composites since the early seventies. [1]

The major constituents used in structuring composites are fibers, particles, laminas, flakes and matrices. The matrix can be thought as the "body" constituent. The other four, which can be referred to as structural constituents, determine the character of the composite's internal structure. Because the constituents are intermixed, there are always regions of contiguity, which can be considered analogous to grain boundaries in metals. The regions may be simply interfaces formed by the contacting surfaces, or they may be composed of a distinct, added phase. Examples of interphases are the coating or coupling agent on glass fibers in reinforced plastics and adhesive that bonds together the layers of a laminate.

The most familiar composites are those composed of one or more types of constituents dispersed in a matrix. For example, reinforced concrete consists of a stone-and-sand aggregate and steel rods (fibers) embedded in a matrix of cement. Recently, organic polymer-inorganic oxide composites have been prepared by embedding the inorganic oxides into the polymer matrix [2]. For example, silica/titanium oxides have been embedded into the polyaniline (PAN) or polypyrrole (PP) bulk.

There are two major reasons for the revived interest in composite materials. One is that the increasing demands for better performance in many product areas, especially in the aerospace, nuclear energy and aircraft fields is taxing to the limit our conventional mono-lithic materials. The second reason- the most important for the long run is that the composites concept provides scientists

with a promising approach to designing, rather than selecting, materials to meet the specific requirements of an application.

On an increasing demand, composites are used as starting materials for many compounds, for instance, a highly electrically conducting plastic by introducing copper in the right form (only 4 vol% is needed) with poly (vinylchloride). The wings of aircraft are made of graphite fiber in a woven form in an epoxy resin. It is moulded to shape in an autoclave. A set of parallel fibers in a matrix is very anisotropic solid which can be used to very good effect in certain devices in computer. Metal matrix composites are being developed because the metal as matrix, say Al or Mg for low temperature applications or Ti for the high temperatures, has advantages over thermosetting resins. The principle of compositing materials is also used in a very sophisticated way in microelectronics. One of the important applications of polymer composite as conducting polymer as electrodes in the rechargeable batteries. In such applications, use is made for the electro-chemical reversibility of the polymers acting as electrodes [3]. The use of thermoplastic, linear chain, polymers as the matrix phase promises to satisfy the criteria which we have defined as necessary for advanced structural composites to become major general materials. [4]

1.2 Synthesis of organic polymer-silica nanocomposites

Two techniques are known for synthesizing nanocomposite materials:

(i) Chemical synthesis and

(ii) Electrochemical synthesis.

A widely used chemical process is the oxidative polymerization. Various oxidizing agents are used in this process such as potassium dichromate, ammonium persulphate, ferric chloride, hydrogen peroxide etc. [5-7]. A colloidal solution is used for the polymerization. During dispersion polymerization[8], a monomer, soluble in the reaction medium is converted into polymer which is insoluble under those conditions. Aggregation of growing insoluble polymer chains results in macroscopic precipitation of the polymer. If, however, a steric stabilizer is present in the system, the precipitation may be prevented and a dispersion of polymer particles, typically of submicrometer to micrometer size, is produced instead [9]. The steric stabilizer is usually polymer soluble in the reaction medium. It becomes either physically adsorbed or chemically grafted onto the precipitating polymer. The resulting "hairy" particles are colloidally stable [10,11] and they do not aggregate.

Conventional chemical polymerization techniques have been successfully applied by various research groups for the preparation of sterically stabilized particles of electrically conducting polymers such PP and PAN. [12]

A wide range of polymer composites e.g. poly (oxyethylene) [13,14], poly (vinyl alcohol-co-vinyl acetate) [15], proteins [16] have been reported by various research groups.

In the electrochemical procedure silica-composites are formed by oxidizing the monomer electrochemically in a dispersion of silica. Several techniques viz. potentiostatic, galvanostatic and potential sweep-techniques such as cyclic voltammetry are used for electrochemical polymerization of aromatic

compounds. In potentiostatic technique a constant potential is applied to the working electrode which is sufficient to oxidize the monomers to be polymerized on the electrode. In galvanostatic process, a constant current density is maintained to polymerize the monomers while film thickness can be controlled in the similar way as for potentiostatic technique. On the other hand, cyclic voltammetry involves sweeping the potential between potential limits at a known sweep rate. On reaching the final potential limit, the sweep is reversed at the same scan rate to the initial potential and the sweep may be halted, again reversed, or alternatively continued further. In such experiments cell current is recorded as a function of the applied potential. Polymerization process is carried out in a single compartment cell containing three electrodes viz. working, counter and reference electrodes. Most commonly used working and counter electrodes are usually platinum while the calomel electrode is used widely as reference. The potential of the working electrode is controlled versus the reference electrode, using a potentiostat. The electrochemical preparation of conducting polymers dates back to early attempts of Dall' olio and co-workers [17] who obtained "pyrrole black" on electrochemical oxidation of pyrrole in aqueous sulphuric acid as an insoluble precipitate on a platinum electrode.

Chemical method has some advantages over electrochemical method. The products which are formed as thin layer on the electrode surface, needed to be separated from time to time. Thus, the process is annoying and also time consuming. Moreover, the electrodes and other electrochemical apparatus are highly expensive. In this work, the studied samples were synthesized chemically.

1.3. Characterization of nanocomposites

1.3.1. Chemical composition

Chemical composition can be determined directly by chemical analysis of the composite or by physical methods such as atomic absorption spectroscopy or x-ray crystallography. In a particular organic polymer-silica systems, elemental analysis for C, H, N can be done by any standard method while analysis for silica content may be performed by the well known hydrofluorization method as described in chapter 2, sec-2.3.

1.3.2 Optical microscopy

In comparison to a biological microscope, the optical one differs in the manner by which the specimen is illuminated. In optical microscope, a horizontal beam of light from some light source is reflected by means of plane-glass reflector, downward through the microscope objective onto the surface of the specimen. Some of this incident light reflected from the specimen surface will be magnified in passing through the lower lens system, the objective and will continue upward through the plane-glass reflector and be magnified again by the upper lens system, the eyepiece. The initial magnifying power of the objective and the eyepiece is usually engraved on the lens mount. When a particular combination of objective eyepiece is used at the proper tube length, the total magnification is equal to the product of the magnifications of the objective and the eyepiece.

The maximum magnification obtained with the optical microscope is about 2000X. The principal limitation is the wavelength of visible light, which limits the resolution of fine detail in the optical specimen. The magnification may be extended somewhat by the use of shorter-wave length radiation, such as ultraviolet radiation, but the sample preparation technique is more involved. The specimen is polished and etched following normal metallographic practice before taking photograph. In the optical microscope the image is brought into focus by changing the lens spacing.

1.3.3. Infra-red (IR) spectroscopy

Electromagnetic radiation beyond the red end of the visible range is called infra-red (IR) radiation. It extends from about 12,000 cm^{-1}. However, the most frequently used part of this range for organic spectroscopy lies between 4000 cm^{-1} and 650 cm^{-1}.

In IR spectrophotometer the IR radiation is passed alternatively through the sample cell and reference cell and resolved with the help of a monochromator. After passing through the monochromator, the decrease in intensity of the IR radiation at different frequency is measured by the detector and recorded as a graph by the recorder which shows IR spectrum with frequency in wave number or wave length on the horizontal axis and intensity or transmission on the vertical axis.

Basically IR spectroscopy is vibrational spectroscopy. Different bonds between specific atoms (C–C, C = C, C ≡ C, C–O, C = O, C–N, C–Cl, O–H, N–H,

etc.) have different vibrational frequencies in molecules and one can detect the presence of these functional groups in an organic molecule by identifying this characteristic frequency as an absorption band in the infrared spectrum.

1.3.4. Inverse gas chromatography (IGC)

Among the techniques [15] currently available to determine interaction parameters of polymer blends, inverse gas chromatography (IGC) has become increasingly popular due to the convenience and general applicability of this technique [16]. IGC is a versatile technique that can provide detailed thermodynamic information on both the surface and bulk properties of materials over a wide temperature range. The term "inverse" means that the stationary phase of the chromatographic column is of interest, in contrast to conventional gas chromatography. One common observation in IGC studies of polymer blends has been extreme dependence of the measured polymer-polymer interaction parameter on the nature of the probe used [18, 19]. This behaviour was attributed to random mixing of polymer chains in the blend or specific interaction of the probe with one of the blend components [20]. IGC has been applied successfully to the characterization of polymers, clays [21], zeolites [22], carbon fibers [23] glass [24] and various other organic and mineral fillers. It has also been demonstrated to be suitable for the characterization of microporous [22] and macroporous materials [25]. Recently Armes and co-workers prepared organic polymer-silica nanocomposites and characterized them successfully by IGC [26].

1.3.5. Particle size determination

Particle size of solids can be determined by a well known sedimentation method. Sedimentation size analysis depends on the fact that the equilibrium velocity of a particle through a viscous medium, resulting from the action of the gravitational force, is related to the size of the particle by Stoke's law. For spherical particles, Stoke's law may be expressed by

$$D = Ku^{1/2} \tag{1.1}$$

$$\text{where, } K = \left[\frac{18\eta}{(\rho - \rho_0)g}\right]^{1/2} \tag{1.2}$$

and D is the diameter of the spherical particle, u its equilibrium sedimentation velocity, and ρ its density. The fluid medium is characterized by viscosity η and density ρ_0, g is the acceleration due to gravity.

When Stoke's law applies, a particle of equivalent spherical diameter D settles by a distance h in time t according to,

$$D = K\left(\frac{h}{t}\right)^{1/2} \tag{1.3}$$

Consequently, after a given time interval t_i, all particles larger than the corresponding diameter D_i will have fallen below a given uniform suspension of particles. If the initial uniform concentration of particles is C_s g/mL and the concentration after time t_i at distance h, C_t g/mL, then P_i, the weight percent of particles finer than D_i is

$$P_i = 100\frac{C_t}{C_s} \tag{1.4}$$

By obtaining the values C_i after various time the corresponding values of P_i and

D_i may be calculated. This set of (P_i , D_i) data pairs when plotted yields an integral, or cumulative distribution of equivalent spherical particle diameter.

Sedigraph instrument utilizes a beam of low energy x-ray to measure particle concentration in terms of transmittance. Transmittance of x-ray is a function of the weight concentration of the suspended solids. When an x-ray beam is passed through a sample container of rectangular cross-section from a direction perpendicular to one of its sides, the fraction of the incident radiation transmitted through the cell filled with particles dispersed in a liquid is given by

$$I/I_0 = \exp\{-(a_l\phi_l + a_s\phi_s)L_1 - a_cL_2\} \qquad (1.5)$$

where I and I_0 are the transmitted and incident intensities; a_l , a_s and a_c the x-ray absorption co-efficient of the liquid, the particle solids and the cell windows respectively; ϕ_l and ϕ_s, the mass fractions of liquid and solids present in the suspension; L_1 the internal cell thickness in the direction of radiation and L_2 the total thickness of the cell windows. By using the relationship $\phi_l = 1-\phi_s$ and by defining transmittance T as the ratio of the transmission of the cell when filled with samples to its transmissions when filled with pure suspending liquid, there is obtained,

$$T = \exp\{-\phi_s(a_s-a_l)L_1\} \qquad (1.6)$$

$$\text{or} \quad \ln(T) = -A\phi_s \qquad (1.7)$$

where A is a constant for the particular apparatus and suspension components. By collimating the x-ray beam through horizontal slits small in vertical dimensions compared to the sedimentation depth, the values of T measured

after specific time intervals can be used in calculating the particle size distribution, i.e.,

$$P_i = 100\frac{\ln T_i}{\ln T_s} \tag{1.8}$$

where T_s refers to the transmittance of the initial suspension p_i and T_i the weight percent of particles and the transmittance of the suspension after the time interval t_i.

Cumulative mass percent finer vs diameter data allow a straight forward conversion to cumulative number and cumulative area by size. For the i^{th} measurement in a series of measurements of a sample, the equivalent spherical diameter is expressed as D_i and the mass percent of particles finer than D_i is expressed by M_i. The mass percent Mc_i within a class interval is expressed by

$$Mc_i = M_i - M_{i+1} \tag{1.9}$$

where two data points (D_i, M_i) and (D_{i+1} , M_{i+1}) define the i^{th} class boundary. The diameter Dc_i chosen to represent the class interval may be its upper or lower boundary or may be some mid-interval value such as the advantage diameter of the class. Knowing the calculation specific volume, Vc_i (volume per gram of sample) within the i^{th} class using the definition of density as follows,

$$Vc_i = \frac{Mc_i}{\rho} \tag{1.10}$$

The equivalent volume v_e of a single spherical particle of diameter Dc_i is calculated from solid geometry as,

$$Ve_i = 0.167\pi\, Dc_i^3 \tag{1.11}$$

The equivalent number of particles per gram contained in the i^{th} intervals is,

$$Nc_i = \frac{Vc_i}{Ve_i} \tag{1.12}$$

1.3.6. Surface area

The volume of a gas taken up by a solid varies from one solid to another and from one gas to another, and in suggesting that the adsorptive power of a solid depends on the area of exposed surface [27]. Two factors (a) surface area (b) porosity, are now recognized to play complimentary parts in adsorption phenomena in a vast range of solids. It thus comes about that measurements of adsorption of gases or vapours can be made to yield information as to the surface area and the pore structure of a solid.

It is obvious that a solid will possess a large surface area if it exists in form of fine particles. There is an inverse relationship between the specific surface (the surface area of one gram of solid) and its particle size. For an idealized case where the particles are cubes of equal size with an edge length l, the specific surface S, is given by the expression,

$$S = \frac{\sigma}{\rho l} \tag{1.13}$$

where ρ = density of the solid.

large specific surface may arise by (a) aggregation, i.e., the fine particles of powder tends to stick together to a greater or lesser extent or by mere adhesion of particles to one another (b) removal of parts of a parent solid such a manner as to leave pores. The walls of pores will comprise the "surface area" of resultant solid.

1.4. Purpose of the adsorption study

The following information can be obtained in an adsorption experiment:

i) Nature of adsorption, that is whether it is adsorbed physically or chemically and the conditions (temperature, pressure, state of adsorbent etc.) under which the adsorption takes place.

ii) Thermodynamic data regarding the adsorption process. These include the amount of gas adsorbed under various equilibrium pressures at definite temperature.

iii) Specific surface area-surface area of one gram of the substance- by the adsorption process can be measured.

1.5. Techniques of measurement of adsorption

Adsorption may be studied directly, by measuring the quantity of the gas taken up, or indirectly by measuring some physical properties of the solid which changes as adsorption proceeds. In the direct method, the amount of gas adsorbed is measured volumetrically, that is by change in pressure of the gaseous adsorbate due to the adsorption or gravimetrically, that is, by change in weight of the adsorbent. In the present investigation, we have used volumetric method to determine the amount of nitrogen adsorbed on the adsorbent.

1.6. Adsorption isotherm

Brunauer has classified adsorption isotherms into five characteristic types shown in Fig. 1.1. Isotherm, types II, represents multilayer physical adsorption

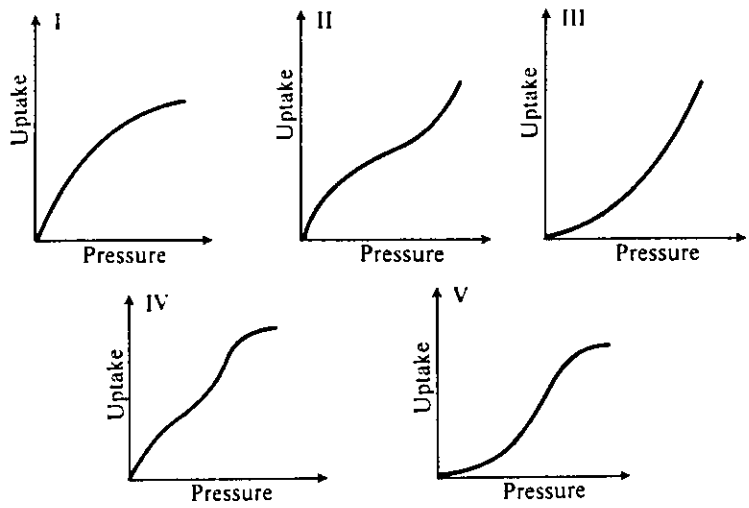

Fig. 1.1. The five adsorption isotherms

on solids. They are often referred to as sigmoid isotherms. For such solids, point B represents the formation of an adsorbed monolayer.

1.6.1. Specific surface area and dispersion measurement

If the composite is not susceptible to poisoning by gases like hydrogen, oxygen or carbon monoxide, the specific surface area of the active component (silica only) can be determined by chemisorption of any of these gases using **Langmuir Isotherm** or the **BET** equation depending on which is appropriate for the given data. If the substance is multicomponent, it is impossible to determine precisely surface area of the individual active components. In that case only the total exposed or active surface area can be determined.

Dispersion of active component: The percentage active component dispersion D_m is given by

$$D_m = \frac{n_w}{n_t} \times 100 \qquad (1.14).$$

Where,

n_w = number of surface active component atoms per unit mass of solids

n_t = total number of active component atoms per unit mass.

The higher is the value of D_m, the higher is the dispersion and the higher will be the activity of catalyst per unit mass of the active component.

Langmuir Isotherm:

Langmuir isotherm may be expressed by the equation

$$\theta = \frac{ap}{1 + ap} \qquad (1.15).$$

where, θ = fraction of the surface covered at equilibrium pressure, p.

a = constant.

The fraction of the surface covered by the adsorbate can be expressed as

$$\theta = \frac{q}{q_m} \qquad (1.16).$$

where,

q = the amount of adsorbate adsorbed at equilibrium pressure, p.

q_m = the amount of adsorbate required to cover the entire surface with a complete monolayer.

Putting the value of θ in equation (1.15), we have,

$$\frac{p}{q} = \frac{1}{q_m \times a} + \frac{p}{q_m} \qquad (1.17)$$

For an adsorbate where the molecule dissociates into two radicals, each occupying a single site, the Langmuir isotherm takes the form

$$\frac{\sqrt{p}}{q} = \frac{1}{q_m \times \sqrt{a}} + \frac{\sqrt{p}}{q_m} \qquad (1.18)$$

From the Langmuir isotherm, the amount of adsorbate required to attain monolayer coverage (q_m) can be found out and thus the number of active sites as well as the surface area per gram of the adsorbent can be calculated using the knowledge of the nature of adsorption (whether it is molecular or dissociative) and the area occupied by per adsorbed particle.

1.6.2. BET equation for multimolecular adsorption

Because the force acting in physical adsorption are similar to that operating in liquefaction (i.e., van der Waals forces), physical adsorption (even on flat or convex surfaces) is not limited to a monomolecular layer, but can continue until a multimolecular layer of liquid covers the adsorbent surface.

The theory of Brunauer, Emmett and Teller is an extension of the Langmuir treatment to allow for multilayer adsorption on non-porous solid surfaces. The BET equation is derived by balancing the rates of evaporation and condensation for the various adsorbed molecular layers and is based on the simplifying that a characteristic heat of adsorption ΔH_1 applies to the first monolayer, while the heat of liquefaction, ΔH_1 of the vapour in the question applies to adsorption in the second and subsequent molecular layers, the equation is usually written in the form

$$\frac{V}{V_{mon}} = \frac{cz}{(1-z)\{1-(1-c)z\}} \qquad (1.19)$$

Where, $z = P/P_0$

V = volume of gas adsorbed in cm^3 per gram of adsorbent at

equilibrium pressure P.

P_0 = saturation pressure of the gas at the temperature of adsorption.

V_m = monolayer capacity, the quantity of the adsorbate which can be accommodate in a completely filled single layer of molecules on the surface of the solid.

c = constant.

With the equation (1.19), it is possible to evaluate V_{mon} from data on adsorption isotherm and from V_{mon} the total surface area can be determined.

Nitrogen is used as the adsorbate (i.e., gas which is adsorbed) at temperature close to the normal condensation point (77K). Under this condition the monolayer of physisorbed molecule is close to packed, resembling a one molecule thick layer of liquid nitrogen covering the entire accessible surface. On this basis the volume occupied by a molecule in the monolayer and in the actual liquid (e.g. liquid nitrogen) phase in presumed to be identical. Thus using the density of this liquid phase in conjunction with the determined amount of gas incorporated into the monolayer, the underlying surface area of the solid may be evaluated. Multiplication of the number of molecules in the monolayer of nitrogen by the area of cross section of the molecule in the liquid nitrogen ($1.62.e^{-19}$) yields the surface area of the solid. An additional feature of adsorption under this condition is that less strongly adsorbed layer tend to develop on top of the initially adsorbed monolayer with approach to saturation pressure of nitrogen (P_0) in a phenomenon known as multilayer adsorption.

1.6.3. Calculation of surface area from BET isotherm

Equation (1.19) can be reorganized into

$$\frac{z}{(1-z)V} = \frac{1}{cVm} + \frac{(c-1)z}{cV_{mon}} \qquad (1.20)$$

It follows that $(c-1)/cV_m$ can be determined from the slope of a plot of the expression on the left (equation 1.20) against z, and cV_{mon} can be obtained from the intercept at z = 0. The results on then be combined to give c and $V_{mon.}$

The number of molecules of nitrogen covering the surface of one gram of adsorbent can be obtained from V_{mon} and c. Since the area of each nitrogen molecule is known (0.16 nm) the total surface area of the solid can be evaluated.

1.7. Review of the literature

Research on nanoparticles has become a wide and interdisciplinary field of science during the last decade. The origin of these efforts may be found in the attempts to photocatalytically split water, which started in the late seventies. Whereas in the pioneering work of Fujishima and Honda [28] suspensions of micrometer-sized TiO_2 were used, researchers soon began to make the particles smaller and smaller. The art of preparing ultra small particles with diameters of only a few nanometers, however, had been neglected during most of the century. Recently, there has been increasing interest in organic-inorganic hybrid materials. Toki *et al* [29] have describe the preparation of poly (vinyl pyrolidine) silica hybrids via sol-gel chemistry. Both Yoshinaga *et al* [30] and Wei *et al* [31, 32] have reported systems in which an organic polymer is

chemically grafted to silica while Zimmermann *et al* [33] have shown that PbS-gelatin nanocomposites can exhibit remarkably high refractive indices. There have also been various papers describing the preparation of composite materials, which contain conducting polymers. Wung *et al* [34] have reported on the preparation and characterization of poly (p-phenylene vinylene)-silica composites and Kramer *et al* [35] have synthesized polyaniline glasses by the in situ chemical polymerization of aniline. Yoneyama's group [36, 37] have incorporated a range of inorganic oxides into electrochemically synthesized thin films of PP and PAN.

Kanatzidis *et al* [38] and other workers have prepared a range of materials in which a conducting polymer is intercalated within an inorganic host matrix. Mayor *et al* [39] reported the preparation of polymer protected palladium nanoparticles and investigated the catalytic activity of the metal polymer system towards the hydrogenation of cyclohexene as a model reaction. Poly pyrrole-tin (iv) systems have been characterized in terms of their particle size, chemical composition, d.c. electrical conductivity and surface composition [40, 41].

1.8 Plan of the present work

Research on nanoparticles has become a wide and interdisciplinary field of science during the last decades. Nanoparticles represent a state of matter in the transition region between bulk solids and molecular structures. Consequently, their physical and chemical properties gradually change from molecular to solid state behavior with increasing particle size. The properties of these novel materials are based mainly on two effects. Firstly, surface properties, i.e., in

particles with diameters of a few nanometers, the number of surface atoms is comparable to those located in the interior crystalline core. Secondly, in the case of metal and semiconductor nanoparticles an additional electronic effect has to be considered. Many exciting experiments have been performed on this novel state of matter with improved materials properties in the fields of luminescence, nonlinear optics, catalysis, electronics, optoelectronics and solar energy conversion.

Following the relevant literature over the last 15 years, it is readily seen that the advances in nanoparticle research were inherently coupled with the availability of high-class materials, i.e., with the progress in the gram scale preparation of well characterized monodisperse particles of various mean sizes and unique surface properties. Recently, preparation of organic polymer-inorganic oxide nanocomposites have been reported. In these works polymers was chemically synthesized by aqueous dispersion polymerization in the presence of ultrafine silica particles. The resulting colloidal mixture was reported to be the nanoscaled composites. Although nanoparticles are expected to exhibit excellent surface properties, to our knowledge, only few reports have appeared on the surface phenomena of the organic polymer-inorganic oxide nanocomposites. Detailed characterization of their adsorption behaviors, surface area measurements etc. have not been made in those reports.

In the present work, it is aimed to focus on searching a new, facile and economic route to synthesize poly(aniline)/silica, poly(*o*-toluidine)/silica and poly(2-chloroaniline)/silica nanocomposites. Instead of using commercial colloidal silica for preparing polymer-silica composites, we report here in the present work, the use of in situ prepared colloidal silica from hydrolysis of

silicate and polymerization of aniline and aniline derivatives to prepare polymer silica composites. The materials were characterized by measuring their physical and chemical characteristics.

References

1. Serafini, T. T., Delvigs, P., and Lightsey, G. R., *J. Appl. Polym. Sci.*, **16,** 905 (1972).
2. Armes, S. P., Intrinsically Conducting Polymers: An Emerging Technology, p-35 (1993).
3. Paul, E. W., Ricco, A. J., and Wrighton, M. S., *J. Phys. Chem.*, **89,** 1441 (1985).
4. Cogswell, F. N., New Materials and their Applications, ed. *Inst. Phys. Conf.*, Middle Brough, **P-79** (1987).
5. MacDiarmid, A. G., Chiang, J. C., and Halpern, M., *Mol. Crys. Liq. Crys.*, **121,** 173 (1985).
6. MacDiarmid, A. G., and Somasiri, N. L. D., *Springer series in solid state Sciences,* **63,** 218, (1985).
7. Barrett, K. E., *J (Ed) Dispersion Polymerization in Organic Media, Wiley,* New York, (1975).
8. Napper, D. H., *Polymeric Stabilization of Colloidal Dispersions, Academic Press*, London (1983).
9. Hunter, R. J., *Foundations of Colloid Science*, **Vol. 1**, Clarendon Press, Oxford (1987).
10. Maeda, S., and Ames, S. P., *J. Mater, Chem*, **4(6),** 935-942 (1994).
11. Vincent, B., and Waterson, J. W., *J. Chem. Soc. Chem. Commun.*, **683,** (1990).
12. Eisazadeh, H., Spinks, H., and Wallace, G. G., *J. Polym. Int.*, **37,** 87 (1995).

13. Gospodinova, N., Mokneva, P., Terlemezyan, L., *J. Chem. Soc., Chem. Commun.*, **923** (1992).

14. Eiasazadeh, H., Gilmore, K. J., Hodgson, A. J., Spinks, G., Wallace, G. G., *Colloids Surf.*, **A103,** 281, (1995).

15. Olabisi, O., Robeson, L. M., and Shaw, M. T., *Polymer-Polymer Miscibility Academic*, New York, (1979).

16. Lipson, J. E. G., and Guiller, J. E., in Developments in polymer characterisations, J. V., Dawkins, Ed, *Applied Sciences Publishers, London*, Chap. **2** (1982).

17. Dall'Olio, A., Dascola, Y., and Varcca, V., *Comptes Redus*, **C267**, 433 (1968).

18. Su, C. S., Patterson, D., and Schreiber, H. P., *J. Appl. Polym. Sci.* **20**, 1025 (1976).

19. Doube, C. P., and Walsh, D. J., *Eur. Polym. J.*, **17.** 63 (1981).

20. Everette, D. H., *Trans. Faraday Soc.* **61**, 1637 (1965).

21. Bandosz, T. J., Putyera, K., Jagiello, J., and Schwarz, J. A., *Microporous Mater.*, **1**, 73 (1993).

22. Oberholtzer, J. E., and Rogers, L. B., *Anal Chem.* **41**, 1590 (1969), Miano, F., *Colloid Surf.*, **A110**, 95 (1996).

23. Schultz, J., Lavielle, L., and Martin, C., *J. Adhesion,* **23**, 45 (1987).

24. Tiburcio, A. C., and Manson, J. A., *J. Appl. Polym. Sci.*, **42**, 427 (1991).

25. Carrott, P. J .M., and Sing, K. S. W., *J. Chromatogr.* **406**, 139 (1987).

26. Perruchot, C., Chehimi, M. M., Delamar, M., Lascelles, S. F., and Armes, S. P., *J. Colloid. Interface Sci.*, **193,** 190-199 (1997).

27. Gordman, J. F., *Ph.D. thesis*, London University (1955).

28. Fujishima, A., and Honda, K., *Nature*, **37**, 238 (1972).

29. Toki, M., Chow, T. Y., Ohnaka, T., Samura, H., and Saegusa, T., *Polym. Bull.*, **29**, 653 (1992).

30. Yoshinaga, K., Yokoyama, T., Sugawa, Y., Karakawa, H., Enomoto, N., Nishida, H., and Komatsu, M., *Polym. Bull.* **28**, 663 (1992).

31. Wei, W., Yang, D., and Tang, L., *Makromol. Chem., Rap. Commun.*, **14**, 273 (1993).

32. Wei, Y., Yang, D. C., Tang, L. G., and Hutchins, M. K., *J. Mater. Res.*, **8**, 1143 (1993).

33. Zimmermann, L., Weibel, M., Caseri, W., and Suter, U. W., *J. Mater. Res.*, **8**, 1742 (1993).

34. Wung, C. J., Wijekoon, W. M. K. P., and Prasad, P. N., *Polymer*, **34**, 1174 (1993).

35. Kramer, S. J. Colby, M. W., Mackenzie, J. D., Mattes, B. R., and Kaner, R. B., in *Chemical Processing of Advanced Materials*, ed. Hench, L. L., and West, J. K., Wiley, Chichester, **P-737** (1992).

36. Kawai, K., Mihara, N., Kuwabata, S., and Yoneyama, H., *J. Electrochem. Soc.*, **137**, 1793 (1990).

37. Yoneyama, H., and Shoji, Y., *J. Electrochem. Soc.*, **137**, 3826 (1990).

38. Kanatzidis, M. G., Tonge, L. M., Marks, T. J. Marcy, H. O., and Kannewurf, C. R., *J.Am. Chem. Soc.*, **111**, 4139 (1989).

39. Mayor, A. B. R., Mark, J. E., *Macromol. Rep.*, **A33**, 451 (1996).

40. Terrill, N. J., Growley, T, Gill, M, and Armes, S. P., *Langmluir*, **9**, 2093 (1993).

41. Gill, M., Armes, S. P., Fairhurst, D., Emmett, S. N., Idzorek, G. C., and Pigott, T., *Langmluir*, **8**, 2178 (1992).

Chapter 2
Experimental

2.1 Materials and instruments

Chemicals:

1) Aniline* (E. Merck, Germany)
2) O-toluidine* (E. Merck, Germany)
3) 2-chloro-aniline* (BDH, England)
4) Hydrochloric acid (E. Merck, Germany)
5) Sodium hydroxide (E. Merck, Germany)
6) Ammonium per sulphate (E. Merck, Germany)
7) Sodium silicate or water glass.

All the chemicals were analytical grade and were used directly without further purification. However, estaric items purified by double distillation prior to use.

Solvent:

De-ionised water.

Porbe:

1) Pentane (E. Merck, Germany).
2) Hexane (E. Merck, Germany).
3) Heptane (E. Merck, Germany).
4) Octane (E. Merck, Germany).
5) Nonane (E. Merck, Germany).

Adsorbates:

1) Nitrogen gas (Purity-99.997%, supplied by BOC, Bangladesh limited).
2) Hydrogen gas (Extra pure, generated by Hydrogen-generator, OPGU-1500s, Japan).

Instruments:

1) pH meter (HM-16s, TOA, Japan) with a combination electrode.
2) Hot plate stirrer (Made in Holland).
3) Centrifuge machine (Universal 16A, Hettich, Germany).
4) 100 mesh and 400 mesh seive (Endecotls test sieves limited, England).
5) Digital balance (FR-200, Japan).
6) Natural oven (NDO-450 ND, EYELA, Japan).
7) Controlled heating vacuum oven (Gallencamp, England).
8) Vacuum desiccator (Made in Germany).
9) Rotary pump (D8A, LEYBOLD-HERAEUS, Germany).
10) Diffusion pump (22625 Br, LEYBOLD-HERAEUS, Germany).
11) Vacuum line (glass apparatus, made by chemistry department, Dhaka university).
12) Infra-red spectrophotometer (IR-470, SHIMADZU, Japan).
13) Optical microscope (SWIFTMASTER II, Swift instrument, Inc. Japan).
14) Micromeritics sedigraph (model no. 5100. USA).
15) Gas chromatograph (Gc-14A, SHIMADZU, Japan).

2.2 Preparation of poly(aniline)/silica nanocomposites

The synthetic procedure for preparing PAN/silica described by the early workers [1-3] was employed in the present work with necessary modification. It is described below:

Aqueous silicate solution was made by dissolving 7.5g of sodium silicate (commonly known as water glass) in 800 mL of de-ionized water in a 1L beaker. This solution was then filtered using Whatman filter paper (No. 41). pH of the solution was adjusted to desired values by adding HCl solution. Then 4.71g of ammonium persulphate was added and the temperature was maintained constant at a desired value by using a hot plate stirrer. 1.0 mL aniline was then injected using a 5 mL syringe and it was seen that the reaction mixture turned into deep green colloidal mixture within few seconds. The reaction mixture was stirred well for a few hours and left over night for completion of the reaction. The colloidal mixture was then centrifuged at 5000 rpm by a centrifuge machine for 30 minutes. The resulting dark green sediment was redispersed in de-ionised water and stirred well to remove the free silica. The centrifugation-redispersion cycle was repeated several times in order to remove free silica particles and soluble by-products from the synthesized PAN/silica nanocomposites. A schematic representation for the preparation of PAN/silica nanocomposite is shown in Fig. 2.1. PAN/silica nanocomposite thus obtained was dried at 100^0C under vacuum. Five different samples of PAN/silica were synthesized maintaining pH 3.1, 7.0 and 11.3 and temperatures at 0^0C, 27^0C and 50^0C. CH_3-PAN/silica and Cl-PAN/silica have

also been synthesized at pH 7 and 27^{0}C following the same procedure described above.

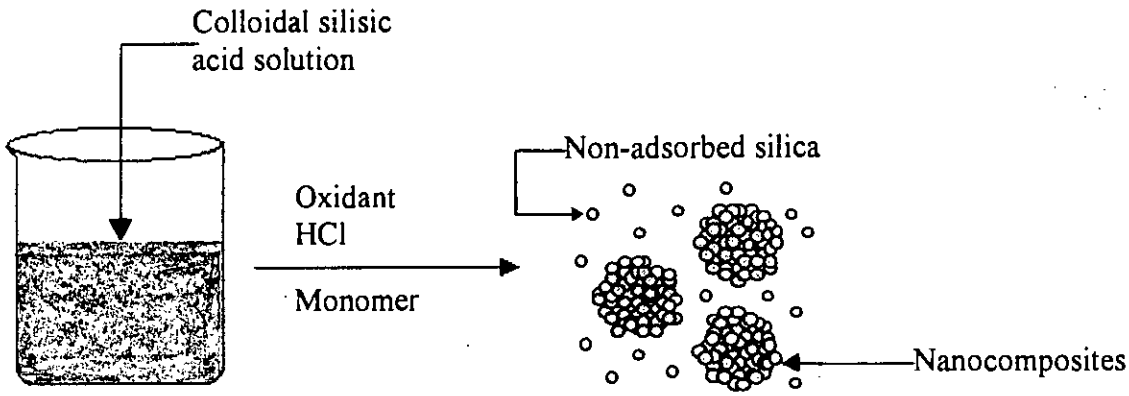

Fig. 2.1. Schematic representation of the formation of organic polymer-silica nanocomposites

2.3 Analysis for silica content

PAN/silica, CH_3-PAN/silica and Cl-PAN/silica were analyzed for their silica content. This was done by the well known hydrofluorization method [4]. About 1g of the sample was taken in a platinum crucible to which 10 mL of HF solution and 1 mL of sulphuric acid solution (1:1) were added. The crucible with lid was placed on a sand bath for evaporation of silica as SiF_4, taking care to avoid loss by spattering. The crucible was cooled, the sides of the crucible washed down with water and 2 mL of HF solution was then added carefully and the contents were evaporated to dryness. The residue was heated on a hot plate until the fumes of sulphuric acid were evolved no longer and then heated in a furnace at 120^{0}C ± 20^{0}C for 15 minutes. The crucible with the residue was

then cooled in a desiccator and weighed. The operation of heating, cooling and weighing were continued until a constant weight was obtained. Each sample was analysed at least thrice and the reported result is the average of the performed runs. The percentage of silica content was calculated as follows:

$$\%SiO_2 = \frac{W_2 - W_3}{W_2 - W_1} \times 100 \qquad (2.1)$$

where, W_1 = mass of the platinum crucible with lid.

W_2 = mass of the platinum crucible with lid plus sample (initially taken)

W_3 = mass of the platinum crucible with lid plus sample (after ignition).

2.4 Optical microscopic analysis

Optical microscopic analysis for the synthesized PAN, PAN/silica, CH_3-PAN/silica and Cl-PAN/silica were performed. For this purpose, samples were compressed to rigid pellet form with a stainless steel dice and a hydraulic press at a pressure of 8-10 tons. Prior to taking the micrographs, all the pellet samples were polished to have a clear and representative view of the sample's microstructure. Polishing was accomplished with emery papers viz. no.3, no.2, no.1, no.0, no.0-0, no.0-0-0 and no.0-0-0-0. In addition to this, wheel polishing with γ-Al_2O_3 powder was also carried out to have better micrograph. After polishing, the samples were cleaned off with dry cotton to remove any traces of polishing materials. Analysis was performed in an optical microscope coupled

with a very high precision canon camera. All the analyses were carried out at room temperature.

2.5 Infra-red spectroscopy

Infra-red (IR) spectra of all the composite materials were recorded on a IR spectrophotometer in the region of 4000-400 cm^{-1}. IR spectra for the solid composites were frequently obtained by mixing and grinding a small amount of the composite materials with dry and pure KBr. Thorough mixing and grinding of the solids were accomplished in an agate mortar. The powder mixture thus obtained was then compressed in a metal holder under a pressure of 8-10 tons to make a pellet. The pellet was then placed in the path of the IR beam in the spectrometer for measurements.

2.6 Particle size determination

Particle sizing of the solids determined by sedimentation method [5] has been reported to be a precision one. In the present work particle size of PAN/silica, CH_3-PAN/silica and Cl-PAN/silica were determined employing a computerized micromeritics sedigraph. For this purpose, samples were ground well in an agate mortar and sieved by a 400 mesh sieve. Density of the sample thus powdered was also determined prior to Sedigraph measurements. Density measurements were accomplished with a pycnometer. A dispersed solution of the sample was then made by taking 2.0g of the powder in 80 mL of water of known density and viscosity. This dispersed solution was then introduced into

the sample holder of micromeritics sedigraph. Data for the particle sizing was made available from the computer interfaced with the Sedigraph.

2.7 Inverse gas chromatography

Inverse gas chromatography (IGC) is a powerful technique [6, 7] for the characterization of composite materials. In the present work IGC was also employed to characterize PAN, PAN/silica, CH_3-PAN/silica and Cl-PAN/silica nanocomposites. For convenience the working procedure divided is into two parts:

a) Packing of column and
b) Chromatographic measurement by a gas chromatograph (GC).

a) **Packing of column:** Prior to packing the samples into the column, these were ground and sieved through 100 mesh sieve. The samples were then placed in the IGC column in such a way that the temperature of the packed mass was maintained uniform. Mica sheet and glass wool were placed on the both ends of the packed column. Two glass rods were kept in pressed at the both ends of the column in order to keep the packed mass undisplaced during the flow of carrier gas and probe through the sample. The column was then placed into chamber of GC, with one end connected to the carrier gas inlet while the other end was connected to the FID detector. The column was a stainless steel tube having a length

of 26 cm and internal diameter of 0.4 cm. A schematic diagram of column is shown in Fig. 2.2.

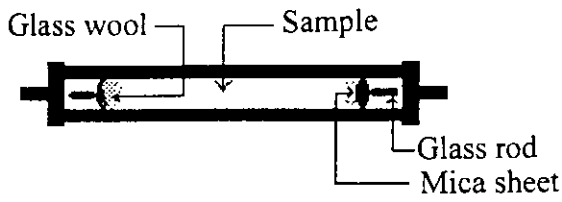

Fig. 2.2. A schematic diagram of column used in IGC

b) **Chromatographic measurement:** This was done by a gas chromatograph fitted with a flame ionization detector (FID). The block diagram of this instrument is shown in Fig. 2.3. A series of alkane, viz.,

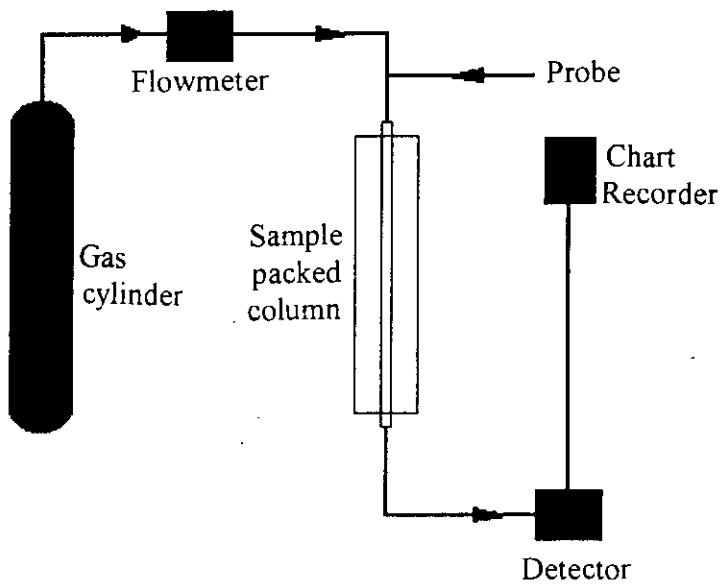

Fig. 2.3. A schematic diagram of IGC instrument

pentane, hexane, heptane, octane and nonane were used as probe and nitrogen gas (99.997%) was employed as carrier gas. The flow rate was maintained at 35 mL min^{-1} as measured by a soap-bubble flow meter. During injection and detection of the studied probes, temperature of the system was maintained at 150^0C. The column was conditioned at 120^0C under a stream of nitrogen gas for 48 hours prior to chromatographic measurements. 0.5μL probe mixture was injected manually by a microlitre syringe. Retention data were recorded graphically at maximum sensitivity. Four stainless steel columns were packed with PAN, PAN/silica, CH_3-PAN/silica and Cl-PAN/silica nanocomposites and their chromatographic measurements were done separately as the procedure described above.

2.8 Adsorption measurements

2.8.1 Pre-treatment of the dry sample

The dried samples were ground with a mortar and a pestler. The ground mass was sieved through a 100 mesh sieve. The powder sample was then taken in a sample vessel and fitted with the adsorption line. The sample was outgassed for 12 hours at 130^0C under high vacuum (about 10^{-6} torr) in order to remove pre-adsorbed gasses as far as possible from the surface of the studied sample. The sample was cooled gradually to room temperature. Prior to adsorption measurement, the sample was cooled further to liquid nitrogen atmosphere.

2.8.2 Apparatus for adsorption measurements

The volumetric method was adopted for measuring adsorption of nitrogen on the studied materials. The adsorbed volume was measured by measuring the change in pressure in the dead space containing the adsorbent. The apparatus consisted of an adsorption vessel and a mercury manometer connected to a conventional high vacuum line made of Pyrex glass (Fig. 2.4). For convenience of description, the apparatus may be divided into three sections,

a) the pumping system

b) the vacuum line and

c) the adsorption system.

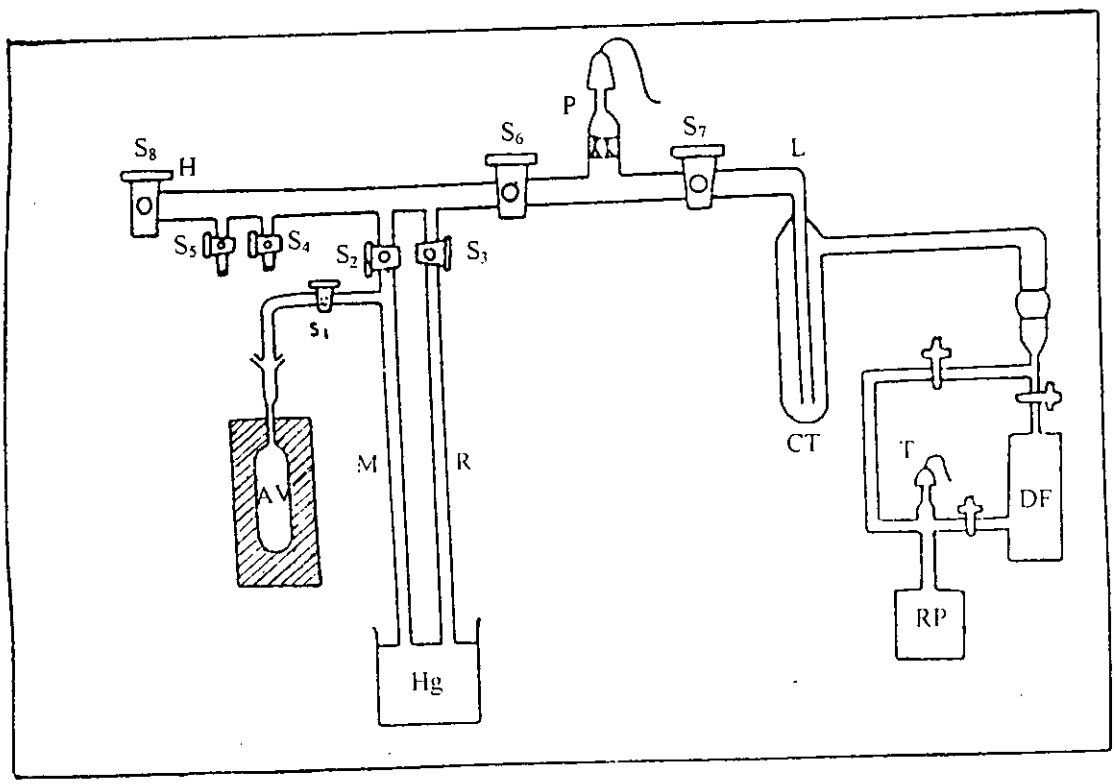

Fig. 2.4. A schematic diagram of high vacuum adsorption line apparatus

a) The pumping system

The pumping system consists of an oil diffusion pump backed by a two stage rotary pump. All connections between the diffusion pump and the rotary pump are made by using small flange fittings and flexible PVC tubing with flanges, appropriate centering rings and perbunan O-rings. For the regulation of pumping path, standard high vacuum valves were used. The backing pressure was monitored by a pirani gauge, T fixed in between the diffusion pump and the rotary pump. A cold trap (CT), maintained at liquid nitrogen temperature, was used to protect the diffusion pump from condensable gases. The line was evacuated to 10^{-2} torr by using the rotary pump while evacuation to 10^{-6} torr was done by the diffusion pump.

b) The vacuum line

The vacuum line consists of a Pyrex glass tubing (HL) of internal diameter 15 mm and it is connected to the pumping system via cold trap (CT). The connection between the cold trap and the pumping system is made by using a B19 quickfit cone and socket joint. High vacuum Pyrex and rotaflow stopcocks are used to separate various sections of the vacuum line for the convenience of adsorption measurement. For the measurement of pressure inside the vacuum line, an ionization gauge (Penning) P, was attached to the line. Stopcocks S_2, S_3, S_4, S_5, S_6 and S_8 are rotaflow. S_1 and S_7 are high vacuum stopcocks. Nitrogen was introduced into the vacuum line through stopcock S_4.

C) The adsorption system

The adsorption system consists of the adsorption vessel, AV and the mercury manometer, M which is connected to the vacuum line. The adsorption vessel is connected to a side of the measuring arm of the

manometer, with the help of the stopcock S_1, such that the adsorption vessel can be isolated from the manometer. The total volume of the adsorption vessel and the side arm up to this stopcock was determined by filling with distilled water before sealing the side arm of the manometer. This volume served as the calibration volume for the measurement of the volume of dead space. The neck of the adsorption vessel was filled with glass wool to prevent the spattering of the powdered sample during evacuation.

R is the reference arm of the manometer, which can be isolated from the vacuum line with the stopcock S_3. The manometer arm and the reference arm of the manometer were made of capillary tubes of internal diameter 0.07 cm. The two arms are dipped in a mercury reservoir (Hg). A porcelain scale, graduated up to 1 mm was placed at the back of the manometer arm for monitoring the pressure. The reference arm was first evacuated so that the height of the mercury level in it is the atmospheric pressure in cm-Hg. The pressure in the adsorption vessel was measured by noting the position of the mercury levels in the two arms with a cathetometer, which allowed to read the position of the mercury meniscus up to 10^{-3} cm. The difference between the readings of the two arms gave the pressure of the gas inside the adsorption vessel.

A tube furnace was used to maintain the adsorption vessel at any desired temperature. The furnace was constructed by winding nichrome wire around a stout Pyrex tube. Winding was done very carefully in order to maintain uniform temperature throughout the furnace. The wire was insulated both thermally and electrically by pasting a thick layer of asbestos cement around it. The diameter of the furnace was just enough to permit comfortable insertion of

the adsorption vessel and a thermometer. For further insulation, after the insertion of the AV and the thermometer in the furnace, the open end of the furnace was covered by a piece of asbestos sheet. The temperature of the furnace was controlled by regulating the current flowing through it with the help of a variable voltage transformer (Variac). The current was monitored by an ammeter included in the circuit.

The furnace was used both for degassing the adsorbent prior to each run and for maintaining the appropriate temperature for a particular run. The temperature of the furnace was measured with a 510°C mercury thermometer, graduated upto 1°C, whose bulb was placed near the sample in the AV. By careful operation of the variac, the constancy of the temperature was possible to maintain in the range ± 2°C.

2.8.3 The adsorbates

Nitrogen and Hydrogen gasses were used as adsorbates in this study. Commercially available highly pure nitrogen gas was allowed to enter the high vacuum line directly without further purification.

The adsorbate hydrogen gas was prepared with commercial equipment which generated pure and dry hydrogen by electrolysis of water. It was introduced directly into the vacuum line without further treatment.

2.8.4 Dead space measurement

Dead space or dead volume is the volume from which the adsorbate is adsorbed on the adsorbent during adsorption measurement. The amounts of gas

adsorbed by the adsorbent is determined by noting the pressure of the gas in the dead space before and after the adsorption and then applying the gas law. For this purpose the volume of the dead space was determined with care.

For measurements of adsorption of nitrogen at 75K on the compostite materials, a large dosing volume as well as a large dead space was necessary, since large amounts of gases are adsorbed under such conditions. In Fig.2.4, the volume within the AV plus the volume between the stop-cocks S_1 and S_2 and the volume in between the stop-cork S_2 S_3 S_6 S_8 S_5 S_4 and top of the mercury meniscus constitute the dead space. The volume of the adsorption vessel AV was determined by weighing the distilled water necessary to fill it and adding this volume with the volume occupied by the side arm upto the stopcock S_1 to evaluate the calibration volume, c. The volume of the side arm upto the stopcock S_1 was previously determined from the weight of distilled water necessary to fill it before sealing the side arm to the manometer. Since the measuring area of the manometer is a part of the dead space its volume is dependent on the pressure. Let the volume of dead space at certain pressure P_f be V_O . In order to calculate this, the volume 'c' was filled with dry air at a certain pressure P_i. It was then allowed to expand into the previously evacuated (P_2=0) space in the manometer arm of volume (V_O - c) and finally, the pressure in the dead volume after expansion was recorded. The volume of the dead space V_O at pressure P_f (which corresponded the particular mercury level in the manometer) could be calculated readily using simple gas law,

$$c\,P_i + (V_O - c)\,P_2 = V_O\,P_f.$$

$$\text{or, } c\,P_i = V_O\,P_f \text{ (as } P_2 = 0)$$

Table-2.1. Dead volume measurement.

(Calibration volume, c = 43.08cm^3; Room temperature = 304.16 K.)

Ref. Arm	Manometer arm		Initial pressure	Final pressure	Dead volume
(cm) L_1	Initial scale reading (cm) L_2	Final scale reading (cm) L'_2	(cm Hg) $P_i = L_1 - L_2$	(cm Hg) $P_i = L_1 - L'_2$	(mL) V_1
80.745	35.890	61.085	44.855	19.660	115.990
	40.715	65.806	40.030	14.939	115.430
	45.460	67.528	35.285	13.217	115.004
	48.785	68.737	31.960	12.008	114.664
	52.870	70.218	27.875	10.527	114.075

A series of such measurements were made with various initial pressures P_i of dry air. In each case the dead volume V_O corresponding to various final pressures P_f were calculated. Table (2.1) contains the data for dead space measurements and Fig. 2.5 shows its variation with mercury level in the manometer. The plot of dead volume against corresponding scale reading (final manometer reading) produced a straight line whose slope is found to be 0.0657 cm^2. The slope expresses the area of cross section of the manometer capillary bore. Any pressure corresponding to a certain position of mercury level in the manometer also corresponds to a definite dead space and that could be calculated from the slope.

During adsorption experiments the actual dead volume was obtained by subtracting the volume occupied by the sample V_S from this calculated value of

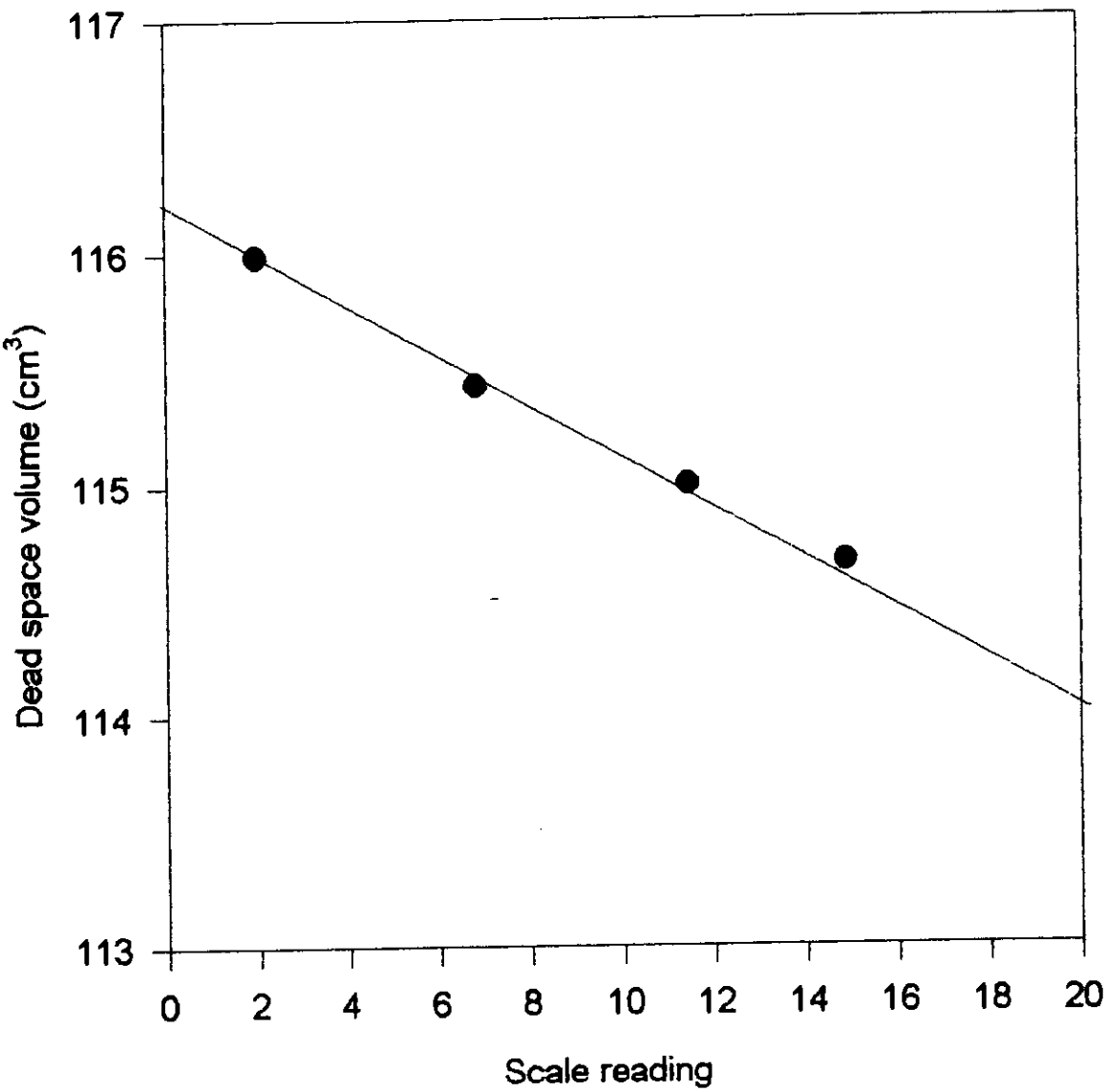

Fig. 2.5: Variation of dead space volume with manometer scale reading

the dead volume V_D. The volume occupied by the sample V_S was calculated by multiplying the mass of the sample and its density.

2.8.5 Method of adsorption measurement

The adsorption was monitored by following the pressure change during the course of adsorption. In a typical experiment, a known amount of the composite materials was taken in the adsorption vessel (AV). Glass wool was placed into the neck of AV to avoid spattering of the sample during initial stage of pumping. The furnace was placed around AV such that the bulb of the adsorption vessel containing the adsorbent and a part of its narrow neck remained in the uniformly heated zone, and the reminder of the neck (with a volume of 9.83 cm^3) was at room temperature. The volume of the adsorption vessel in the transition zone was kept to a minimum, and was not considered in the calculation of gas adsorbed.

Before carrying out adsorption, the sample was degassed by evacuating down to a pressure of 10^{-6} torr. During evacuation the temperature of the furnace was gradually increased upto 403K. Evacuation at 403K was done for four hrs. The temperature of the furnace was then lowered slowly and maintained at the experimental temperature. The evacuated AV was isolated by closing stopcock S_1. Specific treatment of the composite surface was undertaken with specific objectives to investigate the surface of the composite, as will be described later in the results section.

Prior to any gas entry in AV, the rest of the dead space and the vacuum line upto S_8 was flushed several times with the gas to be adsorbed. The space in the

measuring area of the manometer between the stopcocks S_1 and S_2 served as the dosing volume. It was filled with the adsorbate upto a definite chosen pressure.

The definite dose of the adsorbate was then introduced into AV by opening the stopcock S_1 and the pressure in it was monitored at regular time intervals by reading the position of the mercury meniscus in the measuring arm of the manometer with the cathetometer. Equilibrium was considered to have been reached, when no further change in the position of the mercury meniscus could be detected. The stopcock S_1 was closed, and a second dose of the adsorbate was taken in the measuring arm of the manometer, and introduced in the dead space by opening the stopcock S_1. The pressure in the dead space was measured at regular time interval as in the first dose, until equilibrium was attained. Further doses were introduced until no noticeable change in pressure could be recorded. At this stage, the adsobent surface was considered to be saturated with the adsorbed gas.

2.8.6 Treatment of data

By applying the ideal gas equation, the amount of gas adsorbed in each dose was calculated from the measured initial pressure of the dose, and the position of the mercury meniscus in the measuring arm of the manometer which also gave the pressure in the adsorption vessel.

As adsorption was cumulative, the total amount of the gas adsorbed at the end of the adsorption in each dose was found by adding the volume of gas adsorbed in the preceding doses to the volume of gas adsorbed in the current dose.

2.8.7. Calculation of the amount of gas adsorbed

Since adsorption was too rapid, the initial pressure in the dead space (at t = 0) could not be measured directly and the volume of the dead space immediately after dosing the adsorbate was also unknown. The following derivation shows how the initial pressure was obtained by applying ideal gas law and the amount of gas adsorbed was calculated.

In adsorption measurement, a definite dose of the adsorbate was taken in the measuring arm of the manometer and it was then admitted into the dead space by opening the stopcock S_1. The pressure in the adsorption vessel prior to dosing was zero (0) for the first dose, but had a non-zero value, the equilibrium pressure of the previous dose, for the subsequent doses.

Let,

a = Temperature (in K) at which adsorption is measured.

b = Room temperature in K.

c = Volume of the adsorption vessel in cm^3

= 33.08

d = Mass of adsorbent in gram.

t = Volume (cm^3) of that part of the adsorption vessel which was at room temperature = 9.832.

e = Volume of that part of the adsorption vessel which is at the measuring temperature – volume occupied by the adsorbent.

$= c - 9.832 - 0.3759 \times d$

where, specific volume of the silica (major component in the sample) = 0.3759 cm^3/g.

f = Mercury level in the reference arm of the manometer.

g = Manometer scale reading prior to dosing in cm.

v = Manometer scale reading immediately after dosing (t = 0) in cm.

r = Manometer scale reading at any time during adsorption or at equilibrium in cm.

j = Residual pressure of the adsorbate in the adsorption vessel prior to dosing.

V_o = Dead space volume in cm^3 corresponding to zero scale reading of the manometer = $115.49 cm^3$.

Area of cross section of the measuring arm of the manometer

$= 0.0657 cm^2$.

i = Volume of gas taken in the manometer for dosing

$= 115.49 - 33.08 - 0.0657 \times g$

$= 82.41 - 0.0657 \times g. (cm^3)$

h = Pressure of the gas dose = f – g.(cm- Hg)

p = Volume of the part of the dead space in the manometer at t = 0

$= 82.41 - 0.0657 \times v(cm^3)$

n_d = Number of moles of gas dosed = $\frac{h \times i}{R \times b}$ (2.2)

where R is universal gas constant.

n_r = Number of moles of residual gas in the adsorption vessel prior to dosing

$= \frac{9.832 \times j}{R \times b} + \frac{e \times j}{R \times a}$ (2.3)

n_o = Number of moles of adsorbate in the dead space at t = 0

$= \frac{(f - v) p}{R \times b} + \frac{9.832 (f - v)}{R \times b} + \frac{e (f - v)}{R \times a}$ (2.4)

Putting $n_d + n_r$ to n_o, we get a quadratic equation in v:

$$lv^2 + mv + n = 0 \qquad (2.5)$$

Where,

$l = 0.0657 \times a$

$m = (-0.0657 \times a \times f - 17.4717 \times a - b \times e)$ and

$n = 17.4717 \times a \times f + b \times e \times f - h \times i \times a - 9.832 \times a \times j - j \times e \times b = 0.$

Solving the equation (2.5) and discarding the unacceptable root, we get

$$v = \frac{-m - \sqrt{m^2 - 4 \times l \times n}}{2 \times l}$$

Now,

if k = pressure in the dead space at any time or at equilibrium

$= f - r$ (cm- Hg)

S = part of the dead space in the manometer at equilibrium

$= 82.41 - 0.0657$ r.(cm^3)

Then,

n_e = number of moles of adsorbate in the dead space at any time or at equilibrium

$$= \frac{k \times e}{R \times a} + \frac{(S + 9.832)\, k}{R \times b}$$

and no. of moles of gas adsorbed per gram of the adsorbent is given by

$q = (n_o - n_e)/d$ moles per gram adsorbent.

2.8.8. Correction for adsorption on glass wool

Glass wool was employed in the neck of the adsorption vessel to prevent the sample from spattering. It was found that case, adsorption of oxygen or

hydrogen on the amount of glass wool used was insignificant in the temperature range 293-641K and hence no correction was necessary.

References

1. Flitton, R., Johal, J., Maeda, S., Armes, S. P., *J. Colloid Interface Sci.*, **173**, 135-142 (1995).
2. Maeda, S., Armes, S. P., *Langmuir* **11**, No.6, 1899-1904 (1995).
3. Wung, C. J., Wijekoon, W. M. K. P., Prasad, P. N., *Polymer*, **34**, 1174 (1993).
4. Gupta, S. D. and Roy, S. K., *Chemical Analysis of Ceramic and Applied materials*, ed, Gunguly, D. and Kumar, S., *Indian Institute of Ceramics, Calcutta*-700 014, P-38 (1985).
5. Webb, P.A. And Orr, C., *Analytical Methods in Fine Particles*; ed. Micromeritics, USA, P-17 (1997).
6. Lloyd, D. R., Ward, T. C., and Schreiber, H. P. (Eds.), "Inverse Gas Chromatography: Characterization of Polymers and Other Materials", ACS Symposium Series No. 391 *Am. Chem. Soc.,* Washington, DC, 1989.
7. Conder, J. R., and Young, C. L., "Physicochemical Measurement by Gas Chromatography". Wiley, Chichester, 1979.

Chapter 3
Results and Discussion

3.1 General properties of synthesized organic polymer-silica nanocomposites

The preparation of stable colloidal dispersions of conducting polymers using polymeric surfactants/dispersants [1-5] attracted special attention of the material scientists. In the present work sterically and chemically-stabilized conducting polymer particles were synthesized in aqueous medium. We used aqueous silicate solution. It is expected that silica particles prepared in situ from a silicate solution may exist in the nano range when they form stable colloidal nanocomposites with polymers produced simultaneously. Silica grafted polymer nanocomposites were prepared in the pH range 3.1-11.3. PAN, PAN/silica, $-CH_3$-PAN/silica and Cl-PAN/silica have been synthesized in aqueous media by polymerizing the monomers chemically in 1.2 mol L^{-1} HCl solution containing an oxidant. Following the same procedure similar nanocomposites have been reported [6-8] to be synthesized using commercially available colloidal silica as dispersant. A wide variety of oxidant in the chemical polymerization of conducting polymers: H_2O_2 [9], $FeCl_3$ [10] and $(NH_4)_2S_2O_8$ [11] are well established reagents. When aniline is oxidized in the presence of ultrafine silica particles, colloidal PAN/silica nanocomposites are produced. The ultrafine silica sol acts as a high surface-area colloidal substrate for precipitating PAN yielding stable colloidal dispersion of "raspberry" shaped [Fig. 2.1] particles in the range 100-300 nm [6-8]. These colloidal "raspberries" consist of microaggregates of silica "glued" together by the conducting polymer component. PAN absorbs as an insoluble thin layer on to high surface area silica substrate particles. This outer layer of PAN is non-solvated and also acts as a binder. Most of the colloidal silica have a negative

surface charge. Since PAN are poly cations [12, 13], the attractive electrostatic interaction may play a certain role in the formation of PAN/silica particles. Normally one would expect a macroscopic precipitate to be formed in these circumstances. However under certain synthesis condition a stable colloidal dispersion of PAN/silica composite particles were obtained. Similar procedure was found also to be effective for the synthesis of CH_3-PAN/silica and Cl-PAN/silica composites. The chemical analysis of PAN/silica colloids was performed for their silica content. The results have been shown in Table 3.1.1. This analysis indicates that silica content of approximately 11% exists in the chemically prepared polymer/silica composites. Each value was an average of at least three analyses. The result shows that all the samples of PAN/silica, prepared under different conditions, contain almost the same amount of silica. The result also shows that the composites with different functional groups have the same silica content. This finding may suggest that the functional groups do not have any influence on the silica content of the synthesized matrices under investigation. The density values of the samples assessed by pycnometry have also been shown in Table-3.1.1. Each value was an average of at least three runs. The density of the bulk polymer have been found to be smaller than that of polymer-silica composites. This result seems to be reasonable since heavier silica particles having density 2.17 g cm^{-3} are incorporated into the synthesized matrices. Density data observed for the present samples seems to be consistent with the previous reports [14, 15] suggesting that bulk polymer may exhibit lesser density than that of the polymer-silica solids.

These novel composites materials have also been characterized by optical microscope. The micrographs of the synthesized polymer/silica samples are shown in Fig. 3.1.1. Micrograph 3.1.1(a) shows the microstructure of PAN

Table- 3.1.1. Summarized results of chemical analysis and density of the prepared samples.

Name of the sample	Preparation condition		Density ($g\ cm^{-3}$)	Amount of silica (%)
	pH	Temp.(^0C)		
PAN	7	27	1.46	
PAN/silica	7	0	1.765	10.95
PAN/silica	7	27	1.774	11.02
PAN/silica	7	50	1.759	11.05
PAN/silica	3.1	27	1.743	10.92
PAN/silica	11.3	27	1.769	10.99
CH_3-PAN/silica	7	27	1.758	10.98
Cl-PAN/silica	7	27	1.712	11.01

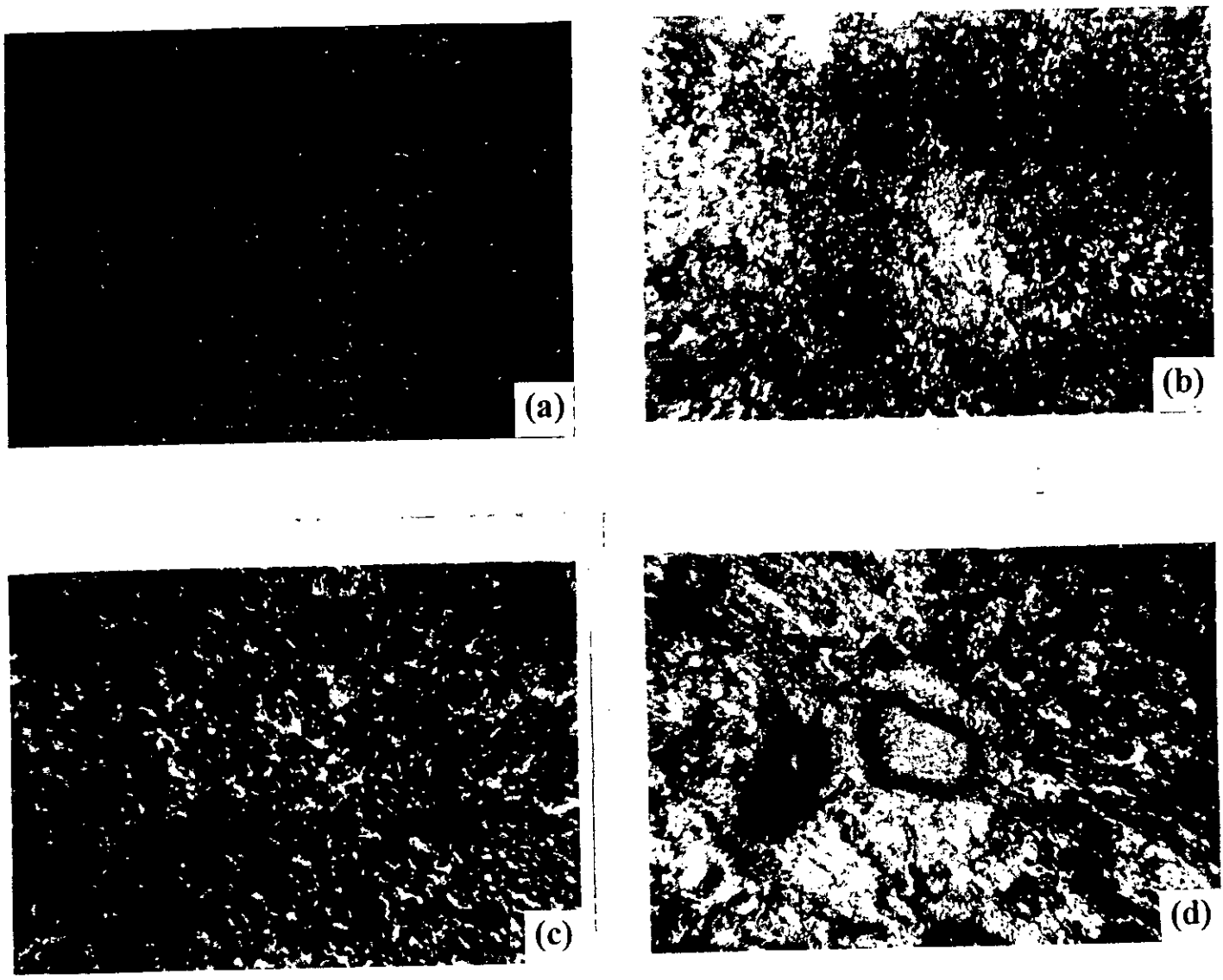

Fig- 3.1.1. Optical micrographs of chemically synthesized (a) PAN, (b) PAN/silica, (c) CH_3-PAN/silica and (d) Cl-PAN/silica (magnification: 1cm ≡3μm).

whereas Fig. 3.1.1(b-d) show the same for PAN/silica, CH_3-PAN/silica, Cl-PAN/silica, respectively. A wide distribution of white images can be seen in the microstructures 3.1.1(b-d). These images may correspond the presence of silica particles in the polymer matrices. It may be considered that their surface composition is silica rich relative to their bulk composition, i.e., the conducting polymer component is probably some what depleted from the surfaces of the particles. This hypothesis has been confirmed for the analogous PP/silica nanocomposites using x-ray photoelectron spectroscopy [15, 16] and zeta potential [18]. Because of the limited magnification of the optical microscope, the free colloidal silica and polymer-silica particles could not be identified separately. However, SEM studies of PP/silica and PAN/silica have been reported to identify clearly the free silica and polymer-silica particles. [14-16]. It is expected that the synthesized composites are free from free silica particles, since synthesis and post-treatment of the synthesized materials were followed exactly as describe by the early workers [6-8]. In the present investigation sedimentometry was employed for sizing the synthesized composites. Owing to the relatively larger density difference between polymer-silica particles and water (0.99 g cm^{-3}), this technique seems to be yielded a better weight-average particle size distributions for PAN/silica as can be seen in Fig. 3.1.2. Considering the simple method used for the synthesis of the present colloidal composite materials, the observed particle size distribution (Fig. 3.1.2) is not narrow rather it shows a broad distribution, indicating the formation of the particles with diameter of different ranges. In fact, particle distributions of PAN/silica, prepared at pH 7 and at 27^0C have been found to be in the range of 40-1 μm. However, the instrumental limitation prevented to detect any formation of PAN/silica particles having diameter below 1μm.

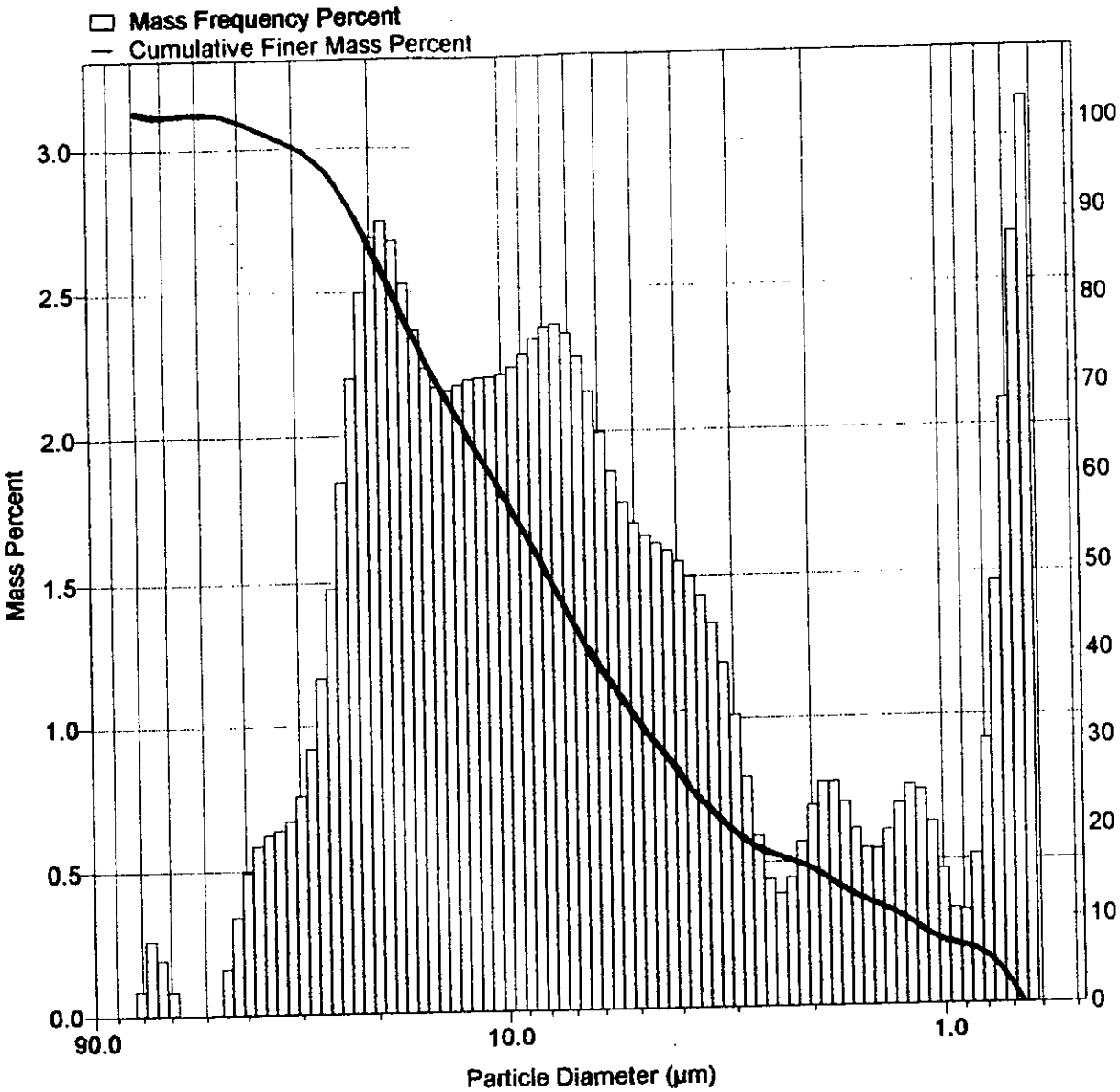

Fig- 3.1.2. Mass frequency versus particle diameter plot for the chemically synthesized PAN/silica.

3.2. IR spectral analysis of chemically synthesized samples

IR spectroscopic studies were carried out in order to get some qualitative information on the synthesized PAN, PAN/silica, CH_3-PAN/silica and Cl-PAN/silica samples. IR spectra of the samples are presented in Figs. 3.2.1-3.2.4 while the observed and standard bands assigned for different functional groups are summarized in Table-3.2.1. The assignment of the bands has been made on the basis of literature data [19-22].

Bands observed in the IR spectrum (Fig. 3.2.1-3.2.4) in the range 3710-3590 cm^{-1} may indicate that water molecules may absorbed by the samples. In fact, De Survill *et. al* [23] have observed that PAN has strong affinity for water, its absorption capacity can be as large as 40% of the polymers weight. The shoulder at 3500-3300 cm^{-1} may correspond the N-H stretching of the aromatic secondary amines. The bands in the range 1690-1640 cm^{-1} may be assigned to C = N- stretching. The presence of this band indicates that the polymer underwent substantial oxidation and is in the form $(C_6H_5 - N = C_6H_5)_n$ may have resulted from the high degree of oxidation of the polymer films [24]. The bands in the range 1600-1450 cm^{-1} and 1350-1250 cm^{-1} may represent C = C and C – N stretching of the aromatic amine, respectively. The bands in the region 900-690 cm^{-1} may provide an evidence for the mono-substituted benzene ring. These findings may indicate that the bonding in the PAN may take place through 1, 2-position. Besides these, the peaks at 2985 and 668 and 744 cm^{-1} for the IR spectrum of CH_3-PAN (Fig. 3.2.3) and Cl-PAN (Fig. 3.2.4), respectively may indicate the presence of $-CH_3$ and –Cl groups in the corresponding polymers. The absorption bands observed in the range 1111-801 cm^{-1} for the samples PAN/silica, CH_3-PAN/silica and Cl-PAN/silica may

Table- 3.2.1. Observed bands and their assignments in the IR spectra of PAN and polymer-silica nanocomposites

Functio-nal groups	Standard absorption band range (cm^{-1})	Observed absorption bands (cm^{-1}) for the samples				Probable assignment
		PAN	PAN/silica	CH_3-PAN/ silica	Cl-PAN/ silica	
Free O–H	3710-3590	3625	3640	3605	3700	O – H stretching vibration water may present
N – H	3500-3300	3338 (sh)	3465 (sh)	3470 (sh)	3465 (sh)	Aromatic secondary amine may present
C = C	1600-1450	1584-1494	1535-1465	1573-1448	1569-1460	C = C stretching in aromatic nucleic.
C – N	1350-1250	1327-1246	1340-1299	1350	1340	C – N stretching in aromatic amine.
C – H	800-690	754-693	788	791-693	793-698	C – H deformation. Monosubstituted benzene.
C = N	1690-1640	1660	1644	1642	1650	C = N stretching in imine
Si – O	1111-801	-	1111-952	1111-960	1111-947	Presence of silica.

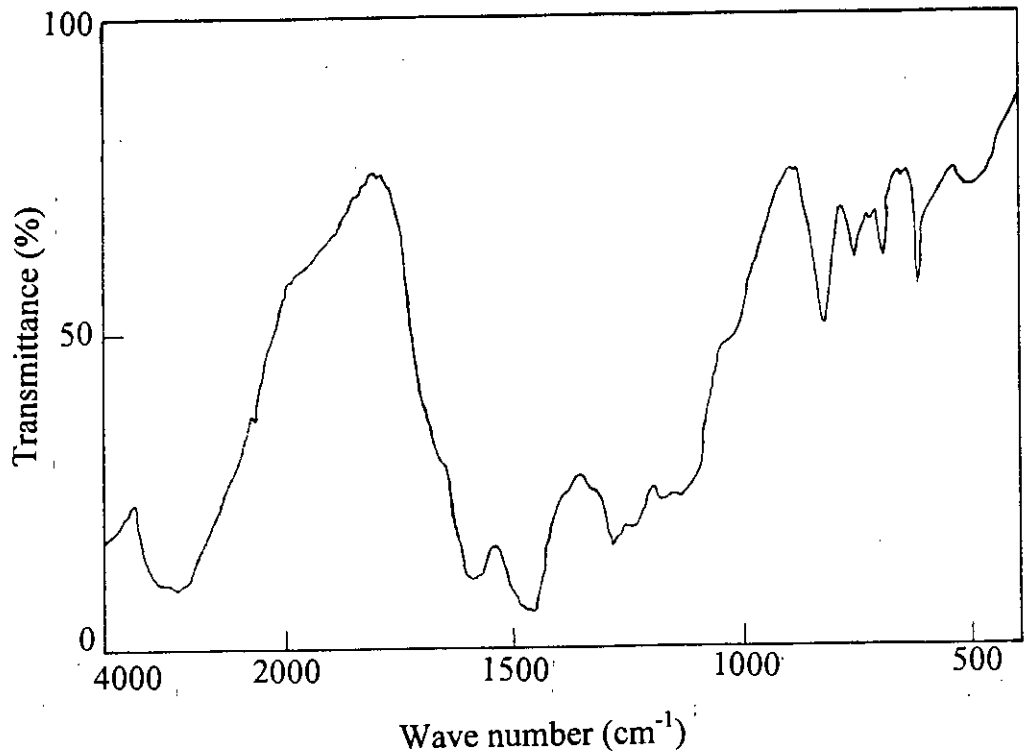

Fig- 3.2.1 IR spectrum of PAN.

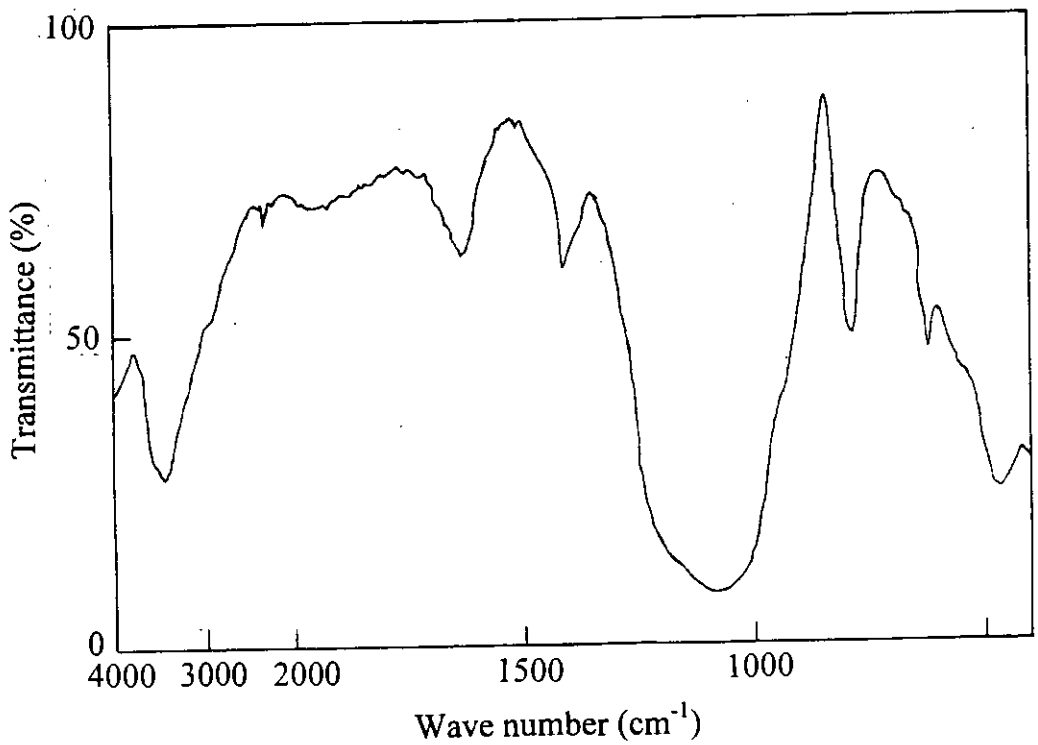

Fig- 3.2.2. IR spectrum of PAN/silica nanocomposite.

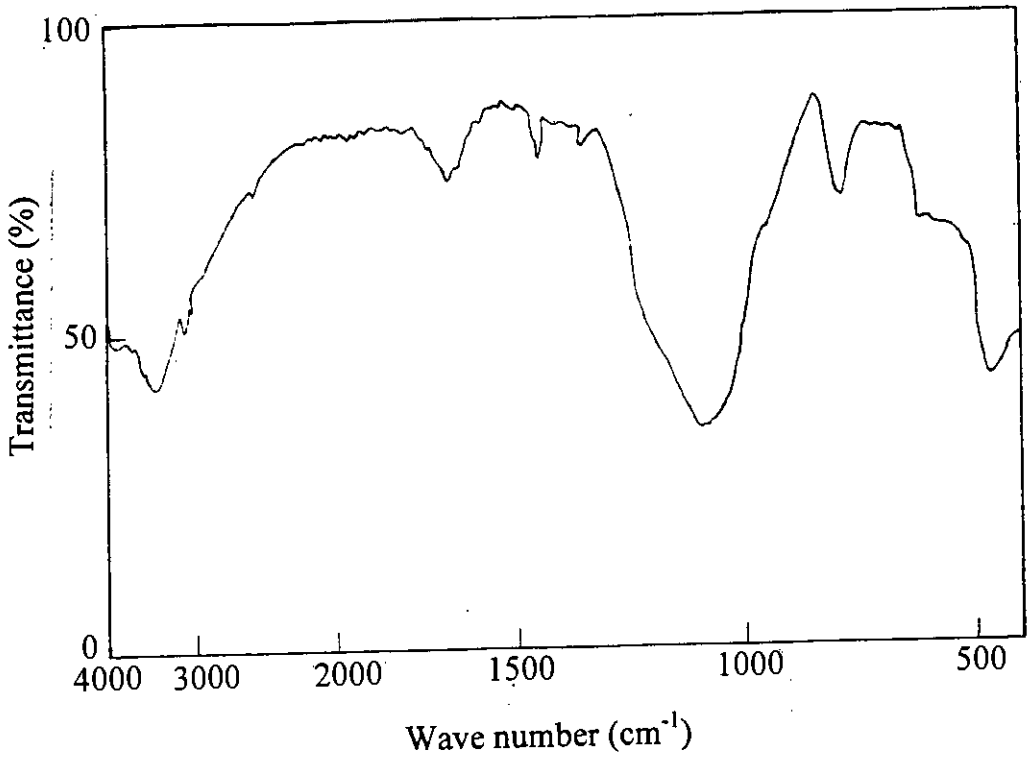

Fig- 3.2.3. IR spectrum of CH_3-PAN/silica nanocomposite.

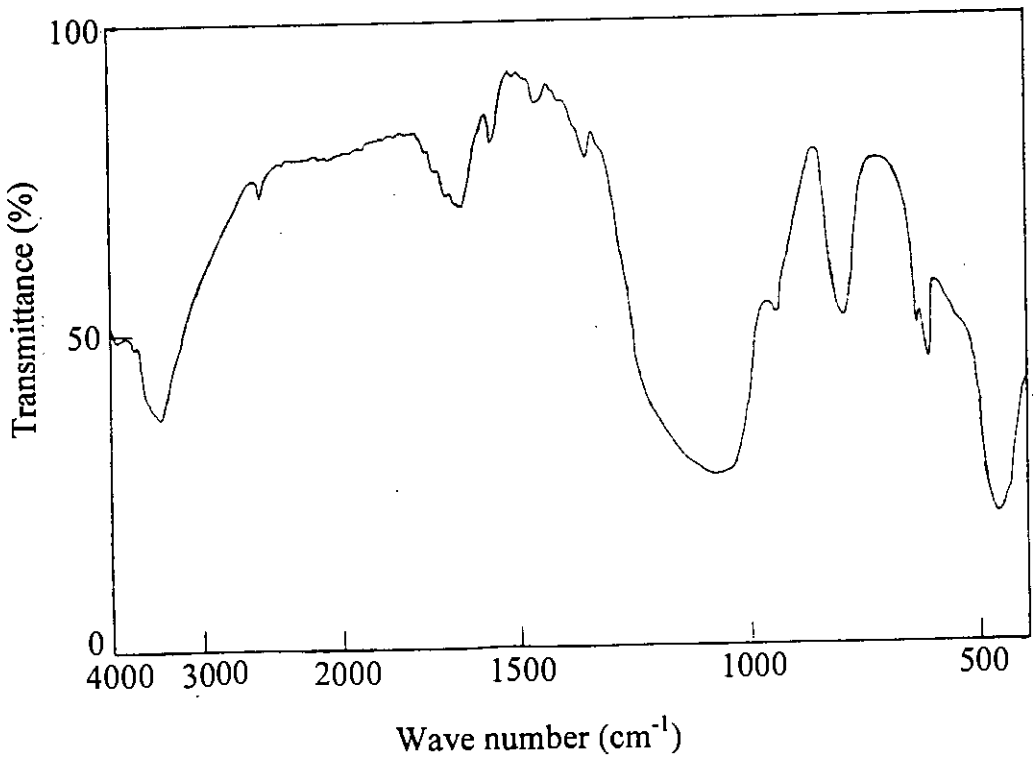

Fig- 3.2.4. IR spectrum of Cl-PAN/silica nanocomposite.

provide evidence for the presence of silica. Therefore, IR spectra of the above studies clearly exhibited adsorption bands attributable to both the polymers and silica components.

3.3. Physico-chemical study of organic polymer-silica nanocomposites by inverse gas chromatography

The present samples synthesized chemically were characterized by IGC. For this purpose, the column was packed with a definite amount of sample. The packed sample was then conditioned at 120^0C with a flow of the carrier gas, N_2 for 48 hours prior to chromatographic measurements.

Liquid probe prepared by mixing equal volume of n-alkanes (C_5-C_9) was employed in the IGC experiments. Typical features of the studied adsorbent and the probes used in the IGC have been exhibited in Table- 3.3.1.

Table-3.3.1: Typical feature of the packed column and IGC probes

Properties of the packed columns			Characteristic of the IGC probes		
Matrices prepared at pH 7 and at 27^0C	Mass (mg)	Length (mm)	Probes	No. of carbon atoms, n_c	Boiling point (^{0}C)
PAN	532	210	n-pentane (C_5)	5	36.1
PAN/silica	531	211	n-hexane (C_6)	6	68.7
CH_3-PAN/silica	536	210	n-heptane (C_7)	7	98.4
Cl-PAN/silica	534	212	n-octane (C_8)	8	125.8
			n-nonane (C_9)	9	150.8

Optimization of operating conditions was made in order to detect each hydrocarbon of the probe. This was done by adjusting various parameters of the operating conditions. These parameters include column initial temperature, column initial time, column final temperature, column final time, programme rate, carrier gas flow rate, injection temperature and detector temperature. On charging 0.5 μL probe into the IGC column, all the five hydrocarbons of the probe were found to be separated at column temperature 120^0C, injection temperature 150^0C and detector temperature 150^0C, carrier gas flow rate 35 $mLmin^{-1}$.

Fig. 3.3.1 exhibits five eluted peaks at different retention time. The present probe also consists of a mixture of five hydrocarbons. It seems from this result that the five eluted peaks may be attributable to the five hydrocarbons of the probe. Therefore, it may be considered that the hydrocarbons are separable with the material packed into the IGC column. Similar finding has also been observed [25] with poly(pyrrole)/silica nanocomposites in separating linear and branched hydrocarbons by IGC technique. It may be mentioned that a silica-supported Pt catalyst with 15% Pt, could not separate the five hydrocarbons from the mixture [26]

Since the probe is composed of series of n-hydrocarbons the elution will depend on their size and boiling points. From this consideration C_5 comes out first, C_6 second and so on. Experiments were performed with the PAN, PAN/silica, CH_3-PAN/silica and Cl-PAN/silica. The sample treatment and the IGC experiment were done in the same way as the procedure described above. All the studied samples have been found to be active in separating the hydrocarbons. Therefore, the materials synthesized in the present work can be

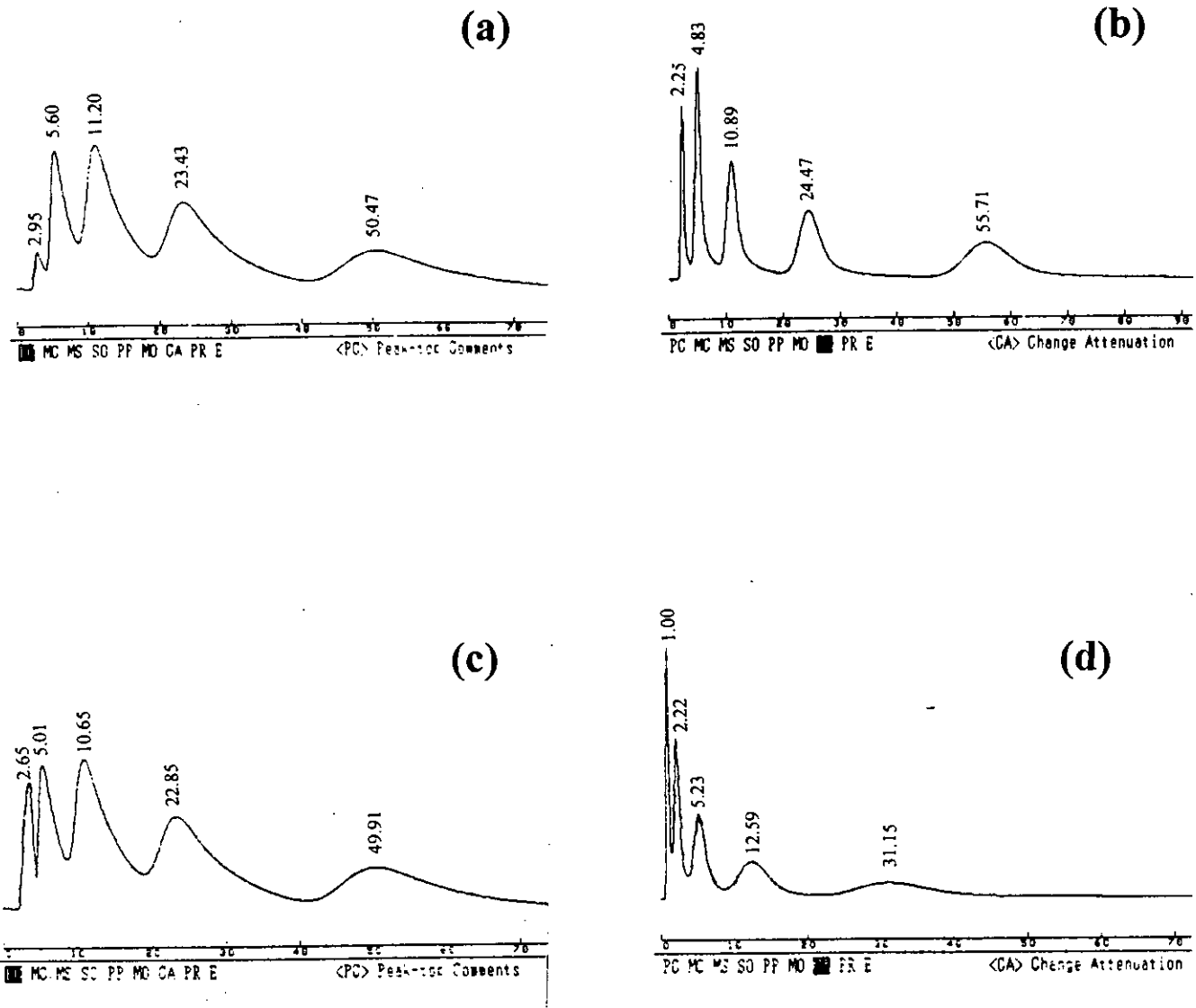

Fig. 3.3.1. Chromatogram for retention time of chemically synthesized (a) PAN, (b) PAN/silica, (c) CH_3-PAN/silica and (d) Cl-PAN/silica.

used as a column material for the separation of hydrocarbons from their mixture.

It is interesting to note that the probe hydrocarbons show different retention time when different adsorbents were used. Among the studied adsorbents for separating the probe hydrocarbons by IGC Cl-PAN/silica matrix shows the lesser retention time while with bulk PAN it is relatively longer. Data for the retention time of the probes is presented in Table- 3.3.2.

Table- 3.3.2: Data for the retention time of the probe for different samples

Sample prepared at pH 7 and at 27^0C	Retention times, t (min)				
	C_5	C_6	C_7	C_8	C_9
PAN	2.95	5.60	11.20	23.43	50.47
PAN/silica	2.25	4.83	10.89	24.47	55.71
CH_3-PAN/silica	2.65	5.01	10.65	22.85	49.91
Cl-PAN/silica.	1.00	2.22	5.23	12.59	31.15

Data Analysis:

In IGC, probes were injected at infinite dilution and behave independently; thus the probe-probe interactions were negligible. Therefore, their retention on the solid surface is governed only by solid-probe interactions. The net retention volume, V_N, is defined as the volume of carrier gas required to sweep out an

adsorbed probe from the chromatographic column. V_N is related to t_N, the net retention time, by

$$V_N = jF\left(1-\frac{p_w}{p_a}\right)\left(\frac{T_c}{T_a}\right)T_N \qquad (3.3.1)$$

Where j is the compression correction factor, F is the carrier gas flow rate measured at the column outlet at ambient pressure (p_a) and temperature (T_a), p_w is the partial pressure of water vapor at T_a, and T_c is the column temperature.

When molecular probes were injected at infinite dilution (zero coverage), ΔG_a, the free energy of adsorption, is related to V_N by

$$-\Delta G_a = RT\ln(V_N) + C \qquad (3.3.2)$$

where R is the gas constant, T is the column temperature, and C is a constant that takes into account the weight and specific surface area of the packing material and the standard states of the probes in the mobile and the adsorbed states [27].

Determination of surface free energy

The purpose of the IGC was to evaluate the dispersive contribution of the samples to the surface free energy, γ_s^d. We have applied the method of Dorris and Gary [28] to γ_s^d using the retention data of the studied n-alkanes series. A plot of ΔG_a or $RT\ln(V_N)$ *vs* the number of carbon atoms in the n-alkanes (n_c) results in a linear correlation, with the slope equal to $\Delta G_a^{CH_2}$, the free energy of adsorption per methylene group. γ_s^d is related to the square of $\Delta G_a^{CH_2}$ by,

$$\gamma_s^d = (1/4\gamma_{CH_2})(\Delta G^{CH_2}/Na_{CH_2}) \qquad (3.3.3)$$

where N is the Avogadro's number, a_{CH_2} is the cross-sectional area of an adsorbed methylene (CH_2) group (6 $A^{0\,2}$), γ_{CH_2} is the surface free energy of a solid comprising only methylene groups such as polyethylene [γ_{CH_2} = 36.8-0.058T] [17].

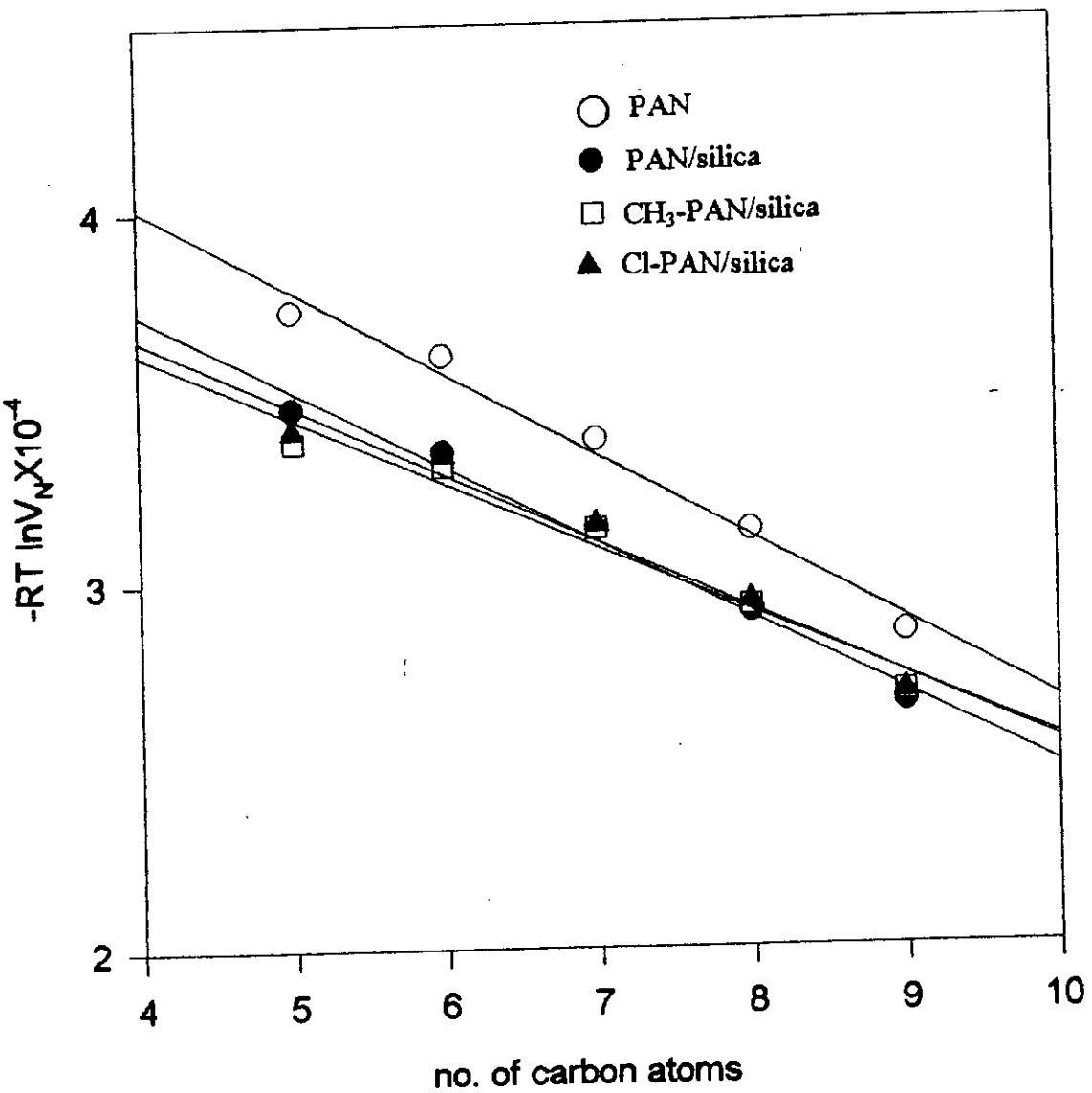

Fig. 3.3.2: RTln(V_N) *vs* no. of carbon atoms for n-alkanes adsorbed onto PAN and composite materials.

Fig. 3.3.2 shows excellent linear plots of RT $\ln(V_N)$ versus the number of carbon atoms generated at 120^{0}C for the PAN, PAN/silica, CH_3-PAN/silica and Cl-PAN/silica. A steeper slope is obtained for the composite materials compared to that of PAN. Therefore, the results may indicate that the composite materials have much higher surface energies than that of PAN. Table- 3.3.3 shows the surface energies of the corresponding materials studied. These findings are in good agreement with the recently published works by Sharaoui *et al* [29] suggesting that the higher surface energy values of composite materials than PAN bulk powder may be due to the microporosity of the composite materials.

Table- 3.3.3: Data for surface energy of the studied samples derived from IGC experimental results

Sample prepared at pH 7 and at 27^{0}C	$\Delta G_a^{CH_2} \times 10^{-3}$	γ_{CH_2}	$a_{CH_2} \times 10^{20}$ m^2	γ_s^d ,mJ/m^2
PAN	1.75	29.84	6.00	17.46
PAN/silica	2.06			24.14
CH_3-PAN/silica	1.84			19.33
Cl-PAN/silica	2.24			28.66

3.4 Measurements of BET surface area

BET surface area measurements of the samples PAN, PAN/silica, CH_3-PAN/silica and Cl-PAN/silica samples were carried out. For this purpose,

nitrogen gas was used as adsorbate. In principle, this technique can provide valuable information regarding specific surface area, average particle size and porosity. Derived BET surface areas of the studied samples are presented in Table-3.4.9 and the results are summarized below:

3.4.1. BET investigation with PAN

The sample PAN was prepared at pH 7 and at 27^0C. The BET measurement was carried out with 0.738g of the sample. For this purpose, adsorption of N_2 on the adsorbent was maintained up to a relative pressure of 0.65. The experimental conditions are shown in Table- 3.4.1. The BET isotherm is shown in Fig. 3.4.1. The monolayer and multilayer regions may be noted in the isotherm. The BET plot seems to be linear as indicated by a very good straight line as can be seen in the Fig. 3.4.2. BET surface area was made from the isotherm. The value obtained was 25.9 m^2g^{-1}. The value is rather low. This finding is not surprising since organic polymer is not known to have high surface area.

Table-3.4.1 : Data for the adsorption of N_2 at 75K on PAN prepared at pH 7 and temperature 27^0C

Experiment number	Equilibrium pressure (cm-Hg)	Relative pressure (P/P_0)	Amount adsorbed (mol g^{-1})x10^4	Surface area (m^2/g)
1	0.0000	0.0000	0.0000	25.9
2	1.3400	0.0176	2.6385	
3	5.7100	0.0751	4.0465	
4	13.0150	0.1712	4.0871	
5	19.7100	0.2593	4.1758	
6	25.8650	0.3403	4.2158	
7	32.1150	0.4226	4.2734	
8	36.7500	0.4836	5.1018	
9	42.1150	0.5541	6.0657	
10	49.2150	0.6476	7.6086	

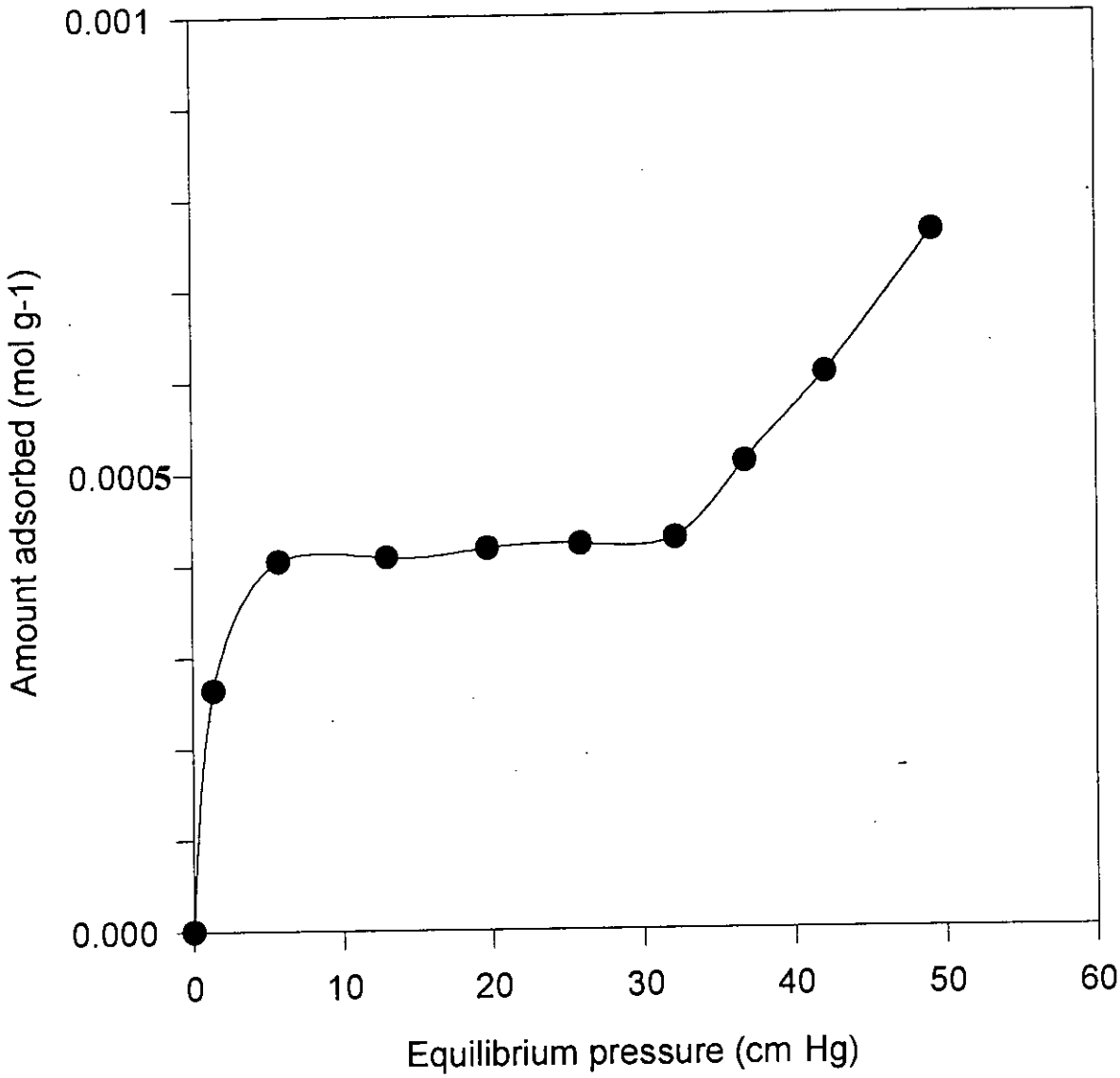

Fig-3.4.1: Isotherm for adsorption of N_2 at 75K on PAN prepared at pH 7 and temperature 27^0C

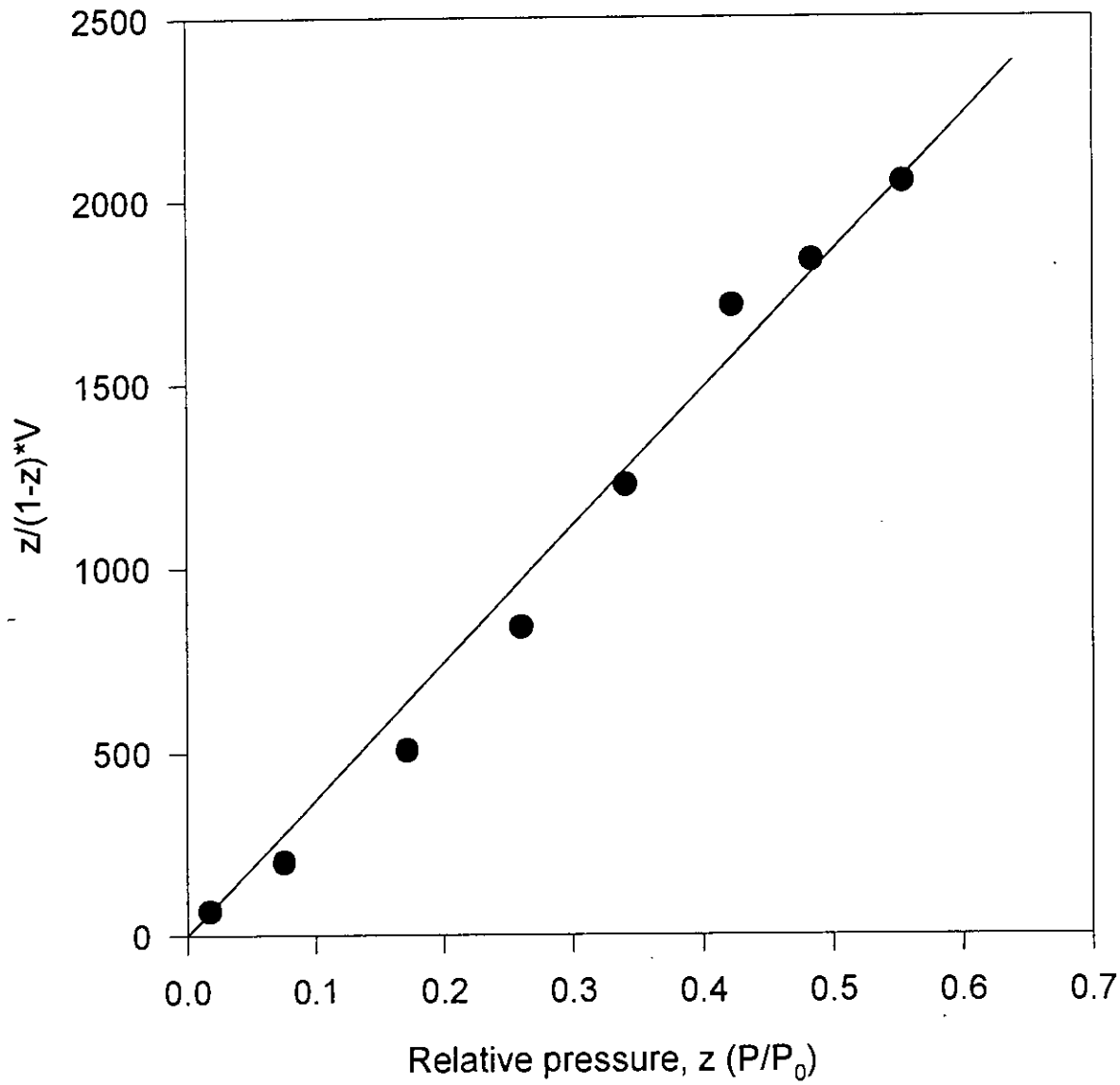

Fig-3.4.2: Linear plot of z/(1-z)*V vs z, where z = P/P_0, according to BET equation for PAN prepared at pH 7 and temperature 27^0C

3.4.2. BET investigation with PAN/silica

Five samples of PAN/silica composites were prepared by varying pH and temperature of the synthesis media. BET surface area of these samples were measured following the procedure as described in section 3.4.1. Experimental data have been summarized in Table- 3.4.2 - 3.4.6. The BET isotherms are also depicted in Fig. 3.4.3, 3.4.5, 3.4.7, 3.4.9 and 3.4.11. The monolayer and multilayer regions are exhibited clearly in the isotherms. The BET plots were presented in Fig. 3.4.4, 3.4.6, 3.4.8, 3.4.10 and 3.4.12. The BET surface area of the studied samples were evaluated and found to be 160.2, 252.7, 184.3, 127.3 and 178.4 m^2g^{-1}.

It can be seen from the results that the PAN/silica composites have higher surface area than that of bulk PAN. The higher surface area of PAN/silica composites may arises due to the incorporation of silica into the PAN matrices. The presence of silica in to the studied composites has been evidenced by chemical analysis, density measurement, optical microscopic and IR spectroscopic analysis as reported previously in section 3.1. It is interesting to note that although all the studied composites contain same amount of silica, their surface area differs greatly. This finding may suggests that, the synthesized composites may differ in porosity and particle size as prepared under different pH and temperature. In fact, Maeda *et. al* [15] reported considerable porosity exhibited by some organic polymer-inorganic oxide nanocomposites. The author also reported BET surface area of PAN/silica nanocomposite as high as 63 m^2g^{-1} which is nearly 4 times smaller than the present PAN/silica samples. The higher surface area observed for the present PAN/silica samples supports further the formation of nanocomposites.

Table-3.4.2 : Data for the adsorption of N_2 at 75K on PAN/silica nanocomposites prepared at pH 7 and temperature 0^0C

Experiment number	Equilibrium pressure (cm-Hg)	Relative pressure (P/P_0)	Amount adsorbed (mol g^{-1})x10^3	Surface area (m^2/g)
1	0.0000	0.0000	0.0000	160.2
2	0.8050	0.0106	0.2225	
3	1.4100	0.0186	0.5566	
4	2.0900	0.0275	1.0887	
5	3.8600	0.0508	1.7148	
6	10.060	0.1324	2.1794	
7	16.090	0.2117	2.4536	
8	21.530	0.2833	2.6542	
9	28.430	0.3741	2.7678	
10	33.425	0.4398	2.9207	
11	38.305	0.5040	3.1640	
12	42.700	0.5618	3.5315	

Table-3.4.3 : Data for the adsorption of N_2 at 75K on PAN/silica nanocomposites prepared at pH 7 and temperature 27^0C

Experiment number	Equilibrium pressure (cm-Hg)	Relative pressure (P/P_0)	Amount adsorbed (mol g^{-1})x10^3	Surface area (m^2/g)
1	0.0000	0.0000	0.0000	252.7
2	0.1850	2.4342e-3	0.2503	
3	0.3850	5.0658e-3	0.6339	
4	0.4450	5.8553e-3	1.2344	
5	2.1800	0.0287	1.9178	
6	7.3050	0.0961	2.4776	
7	12.430	0.1636	2.8308	
8	17.570	0.2312	3.1769	
9	22.605	0.2974	3.5284	
10	27.125	0.3569	3.8943	
11	31.765	0.4180	4.3191	
12	37.300	0.4908	4.9235	
13	42.725	0.5622	6.1864	

Table-3.4.4 : Data for the adsorption of N_2 at 75K on PAN/silica nanocomposites prepared at pH 7 and temperature 50^0C.

Experiment number	Equilibrium pressure (cm-Hg)	Relative pressure (P/P_0)	Amount adsorbed (mol g^{-1})x10^3	Surface area (m^2/g)
1	0.0000	0.0000	0.0000	184.3
2	0.6950	9.1447e-3	0.1597	
3	1.6500	0.0217	0.3907	
4	2.6650	0.0351	0.7067	
5	3.6500	0.0480	1.0981	
6	6.0000	0.0789	1.5298	
7	9.6050	0.1264	1.9697	
8	16.490	0.2170	2.3197	
9	24.350	0.3204	2.5802	
10	30.720	0.4042	2.8649	
11	34.610	0.4554	3.2302	
12	39.600	0.5211	3.7110	

Table-3.4.5 : Data for the adsorption of N_2 at 75K on PAN/silica nanocomposites prepared at pH 3.1 and temperature 27^0C

Experiment number	Equilibrium pressure (cm-Hg)	Relative pressure (P/P_0)	Amount adsorbed (mol g^{-1})x10^3	Surface area (m^2/g)
1	0.0000	0.0000	0.0000	127.3
2	0.1200	1.5789e-3	0.1109	
3	0.6750	8.8816e-3	0.1793	
4	1.0200	0.0134	0.8057	
5	2.1850	0.0288	0.8274	
6	4.8800	0.0642	1.2273	
7	9.2050	0.1211	1.4699	
8	14.145	0.1861	1.7042	
9	21.180	0.2787	1.8658	
10	27.115	0.3568	2.0151	
11	31.340	0.4124	2.2286	
12	36.375	0.4786	2.5333	
13	44.300	0.5829	3.0315	

Table-3.4.6 : Data for the adsorption of N_2 at 75K on PAN/silica nanocomposites prepared at pH 11.3 and temperature 27^0C

Experiment number	Equilibrium pressure (cm-Hg)	Relative pressure (P/P_0)	Amount adsorbed (mol g^{-1})x10^3	Surface area (m^2/g)
1	0.0000	0.0000	0.000	178.4
2	0.6990	9.0447e-3	0.156	
3	1.6671	0.0207	0.390	
4	2.6777	0.0348	0.700	
5	3.6621	0.0473	1.093	
6	6.0123	0.0699	1.524	
7	9.6255	0.1996	1.960	
8	16.498	0.2070	2.310	
9	24.362	0.3184	2.578	
10	30.733	0.4022	2.858	
11	34.625	0.4504	3.220	
12	39.675	0.5177	3.700	

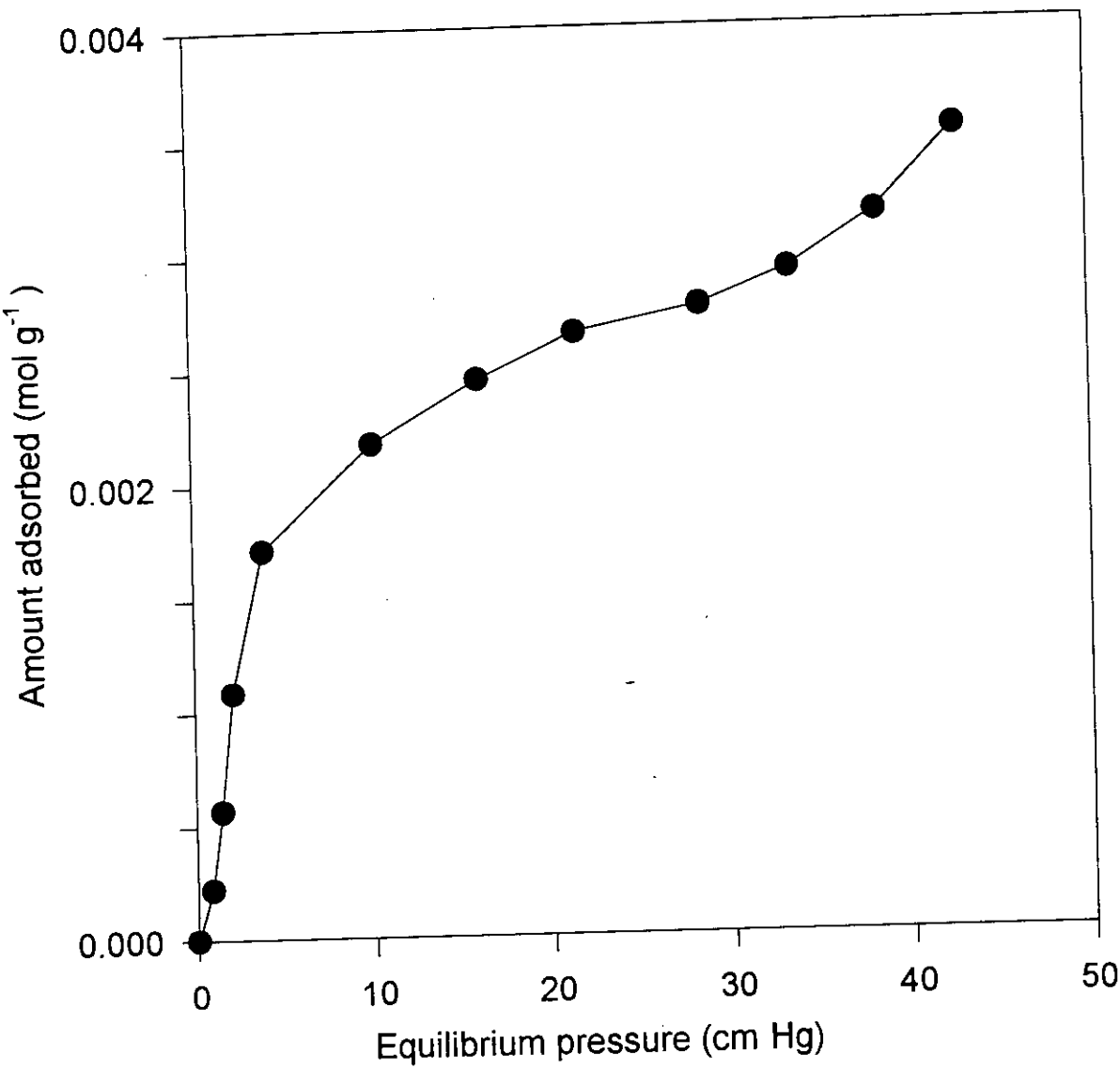

Fig-3.4.3: Isotherm for adsorption of N_2 at 75K on PAN/silica prepared at pH 7 and temperature 0^0C

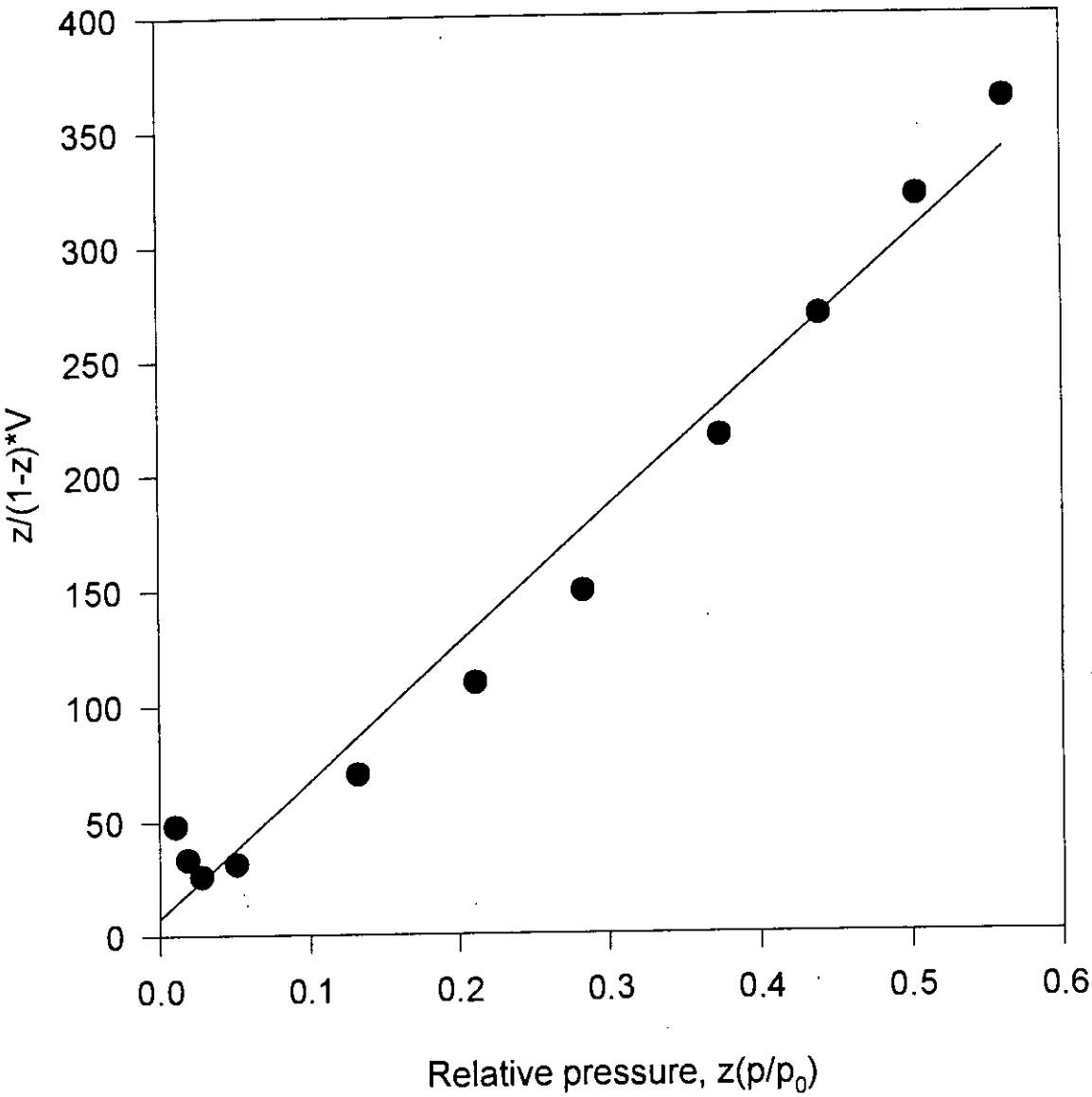

Fig-3.4.4: Linear plot of z/(1-z)*V vs z, where z = P/P_0, according to BET equation for PAN/silica prepared at pH 7 and temperature 0^0C

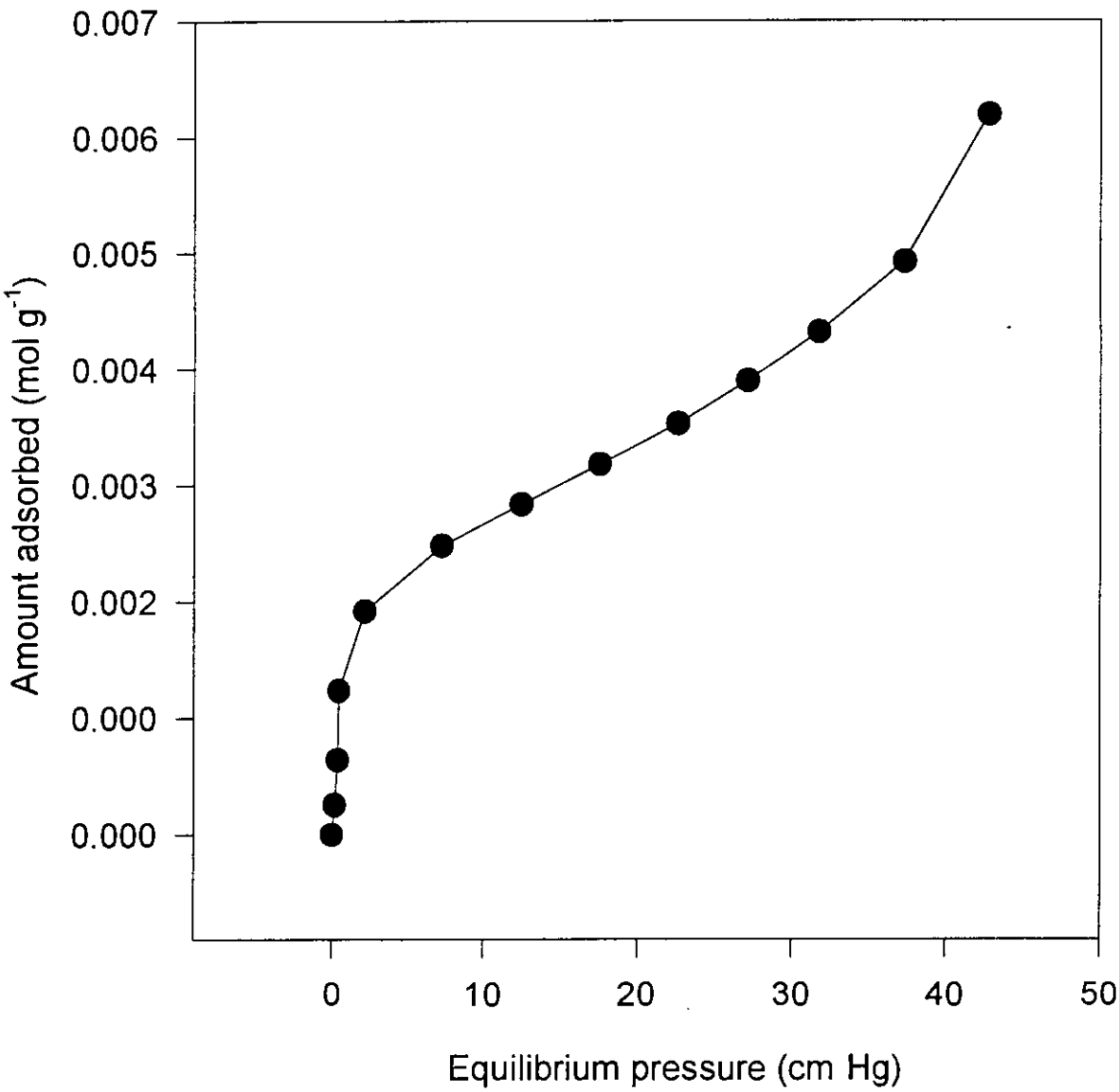

Fig-3.4.5: Isotherm for adsorption of N_2 at 75K on PAN/silica prepared at pH 7 and temperature 27^{0}C

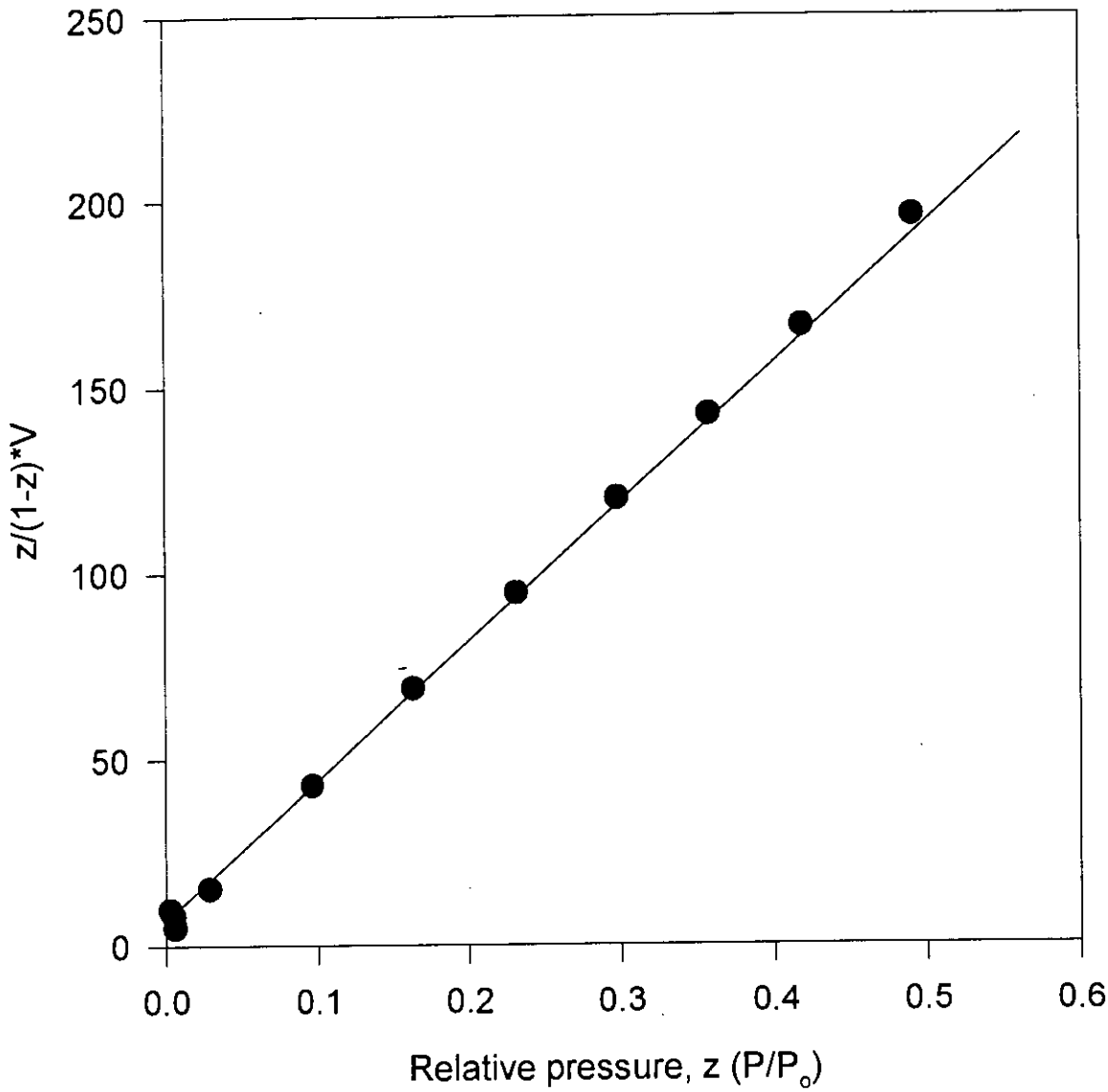

Fig-3.4.6: Linear plot of z/(1-z)*V vs z, where z = P/P_0, according to BET equation for PAN/silica prepared at pH 7 and temperature 27^0C

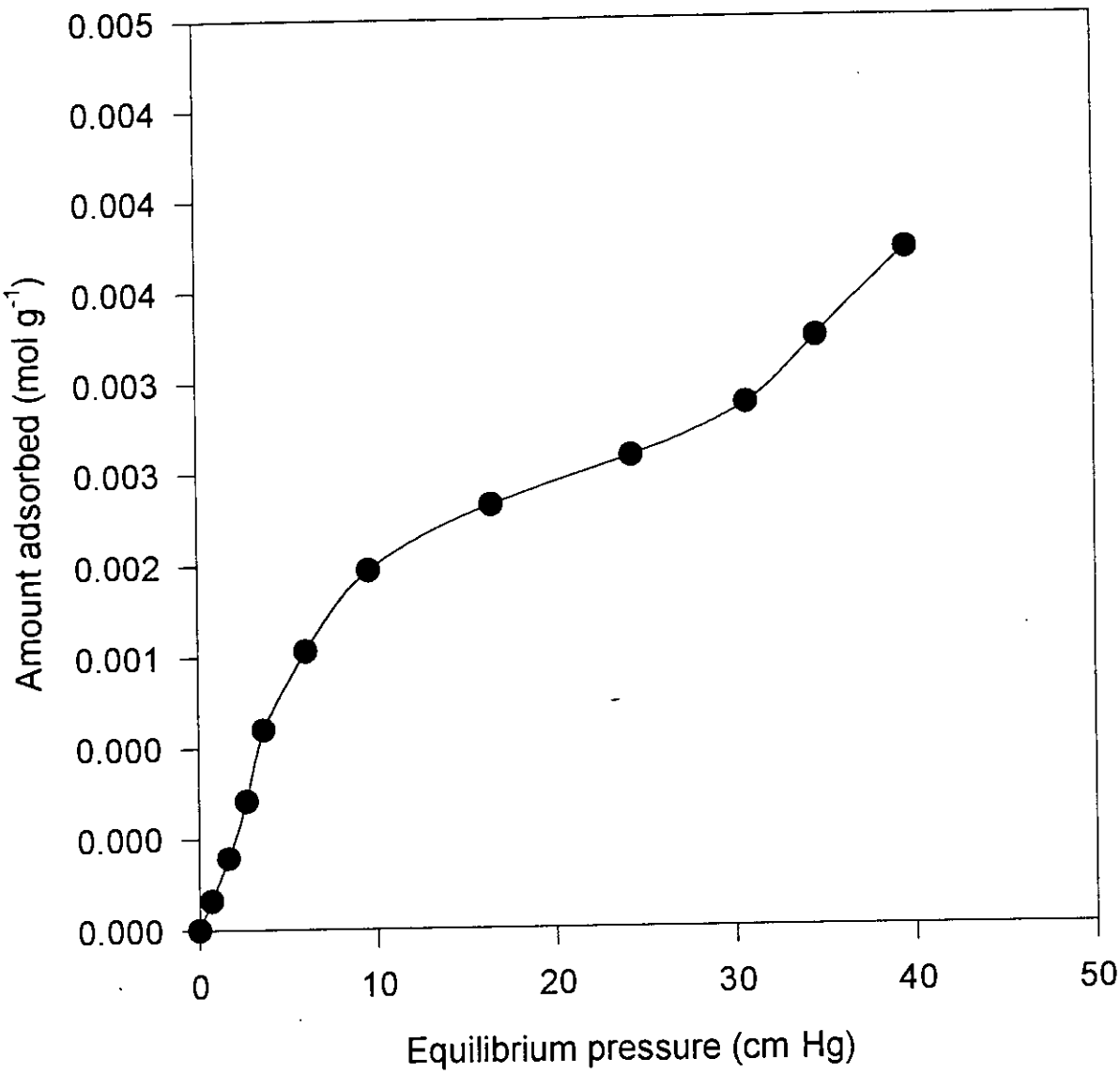

Fig-3.4.7: Isotherm for adsorption of N_2 at 75K on PAN/silica prepared at pH 7 and temperature 50^0C

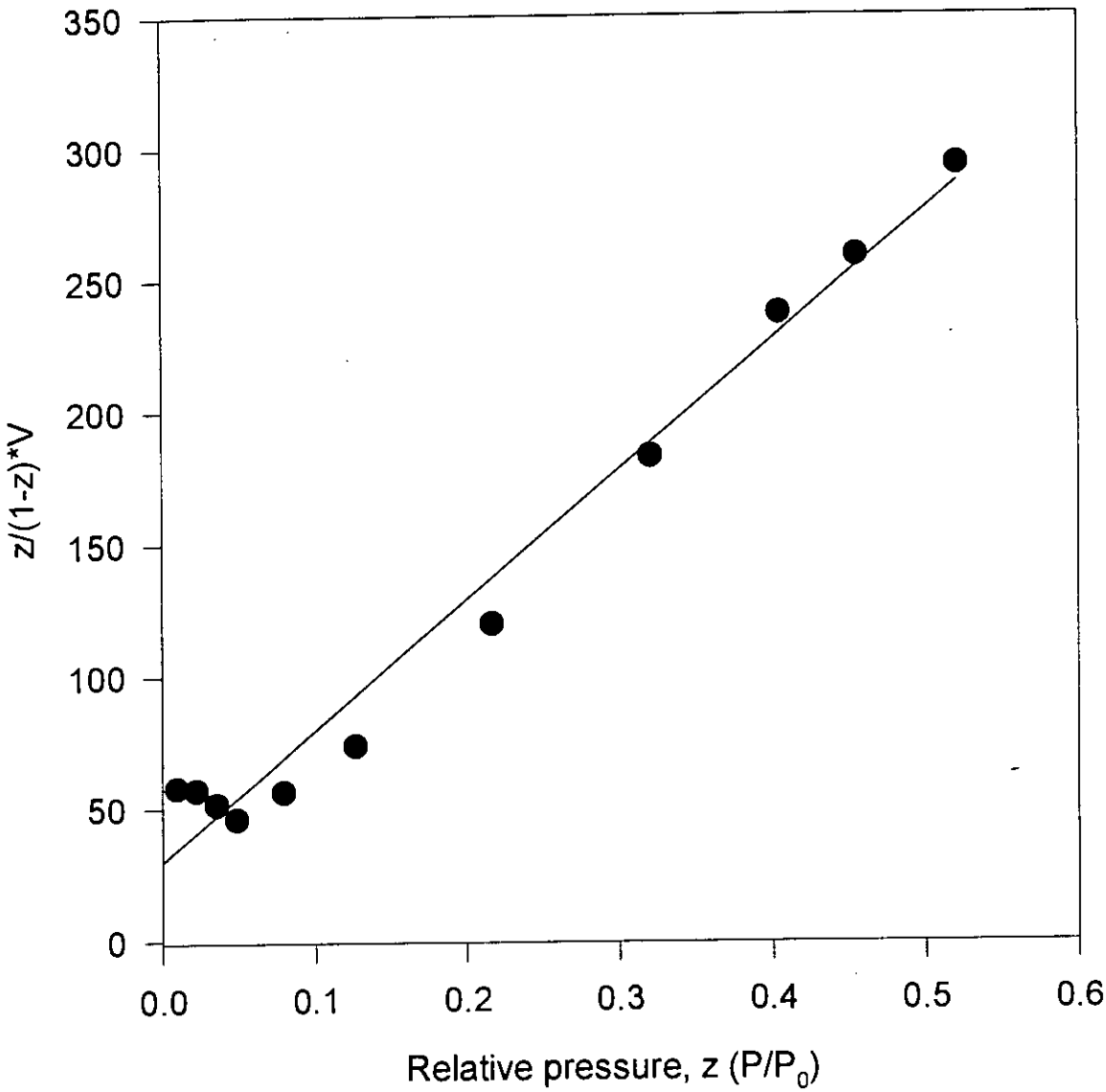

Fig-3.4.8: Linear plot of z/(1-z)*V vs z, where z = P/P_0, according to BET equation for PAN/silica prepared at pH 7 and temperature 50^{0}C

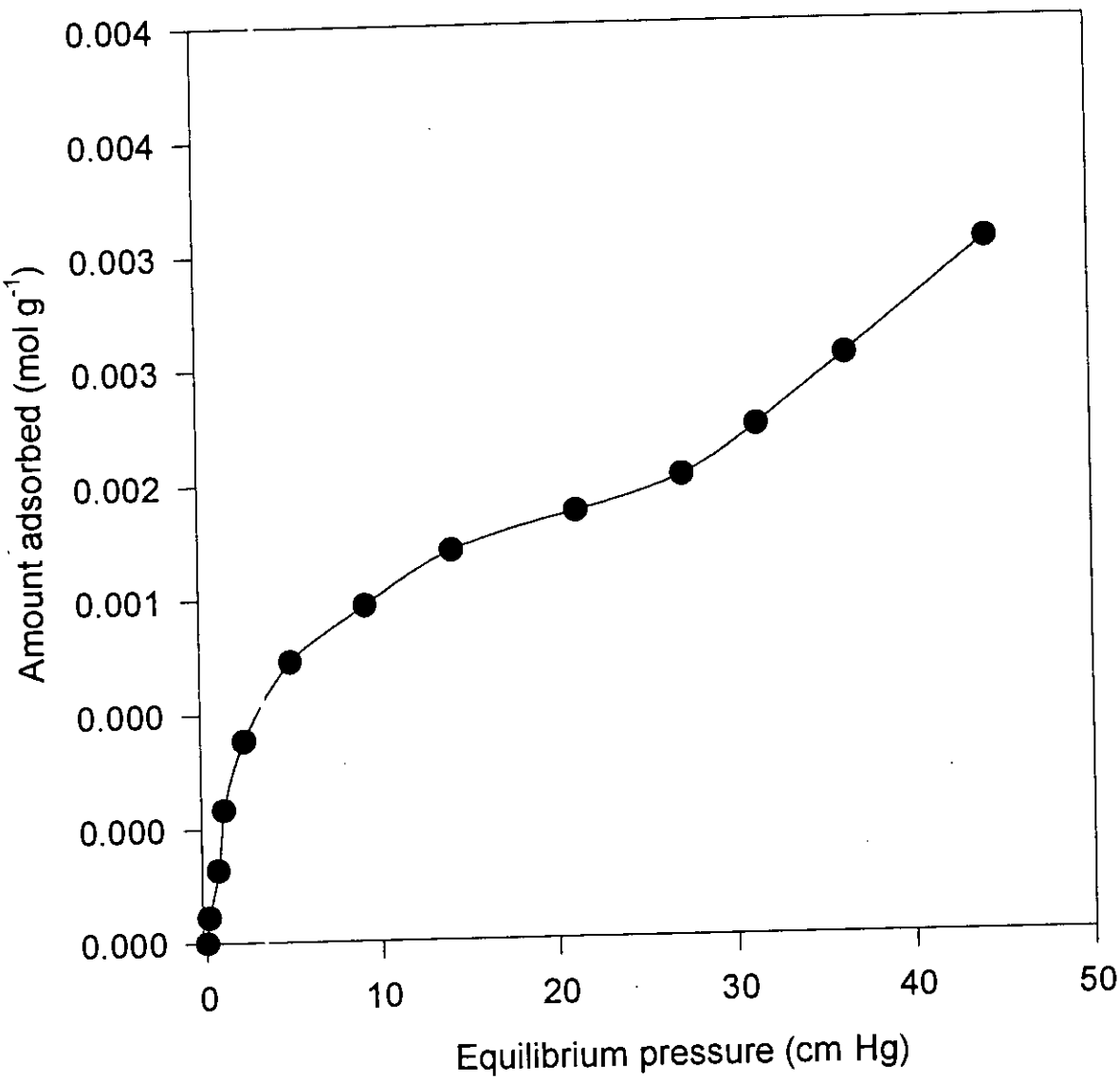

Fig-3.4.9: Isotherm for adsorption of N_2 at 75K on PAN/silica prepared at pH 3.1 and temperature 27^0C

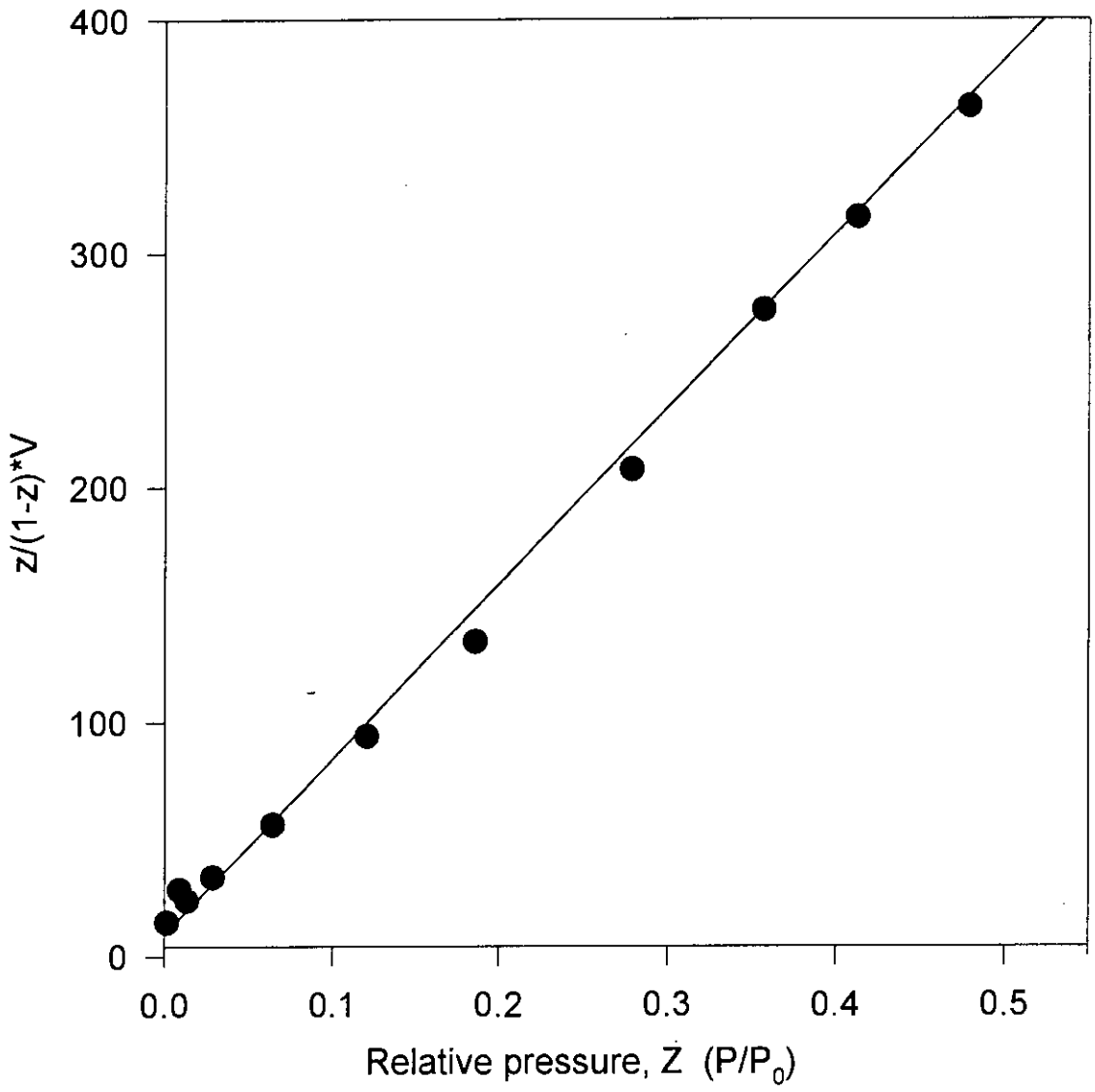

Fig-3.4.10: Linear plot of z/(1-z)*V vs z, where z = P/P_0, according to BET equation for PAN/silica prepared at pH 3.1 and temperature 27^0C

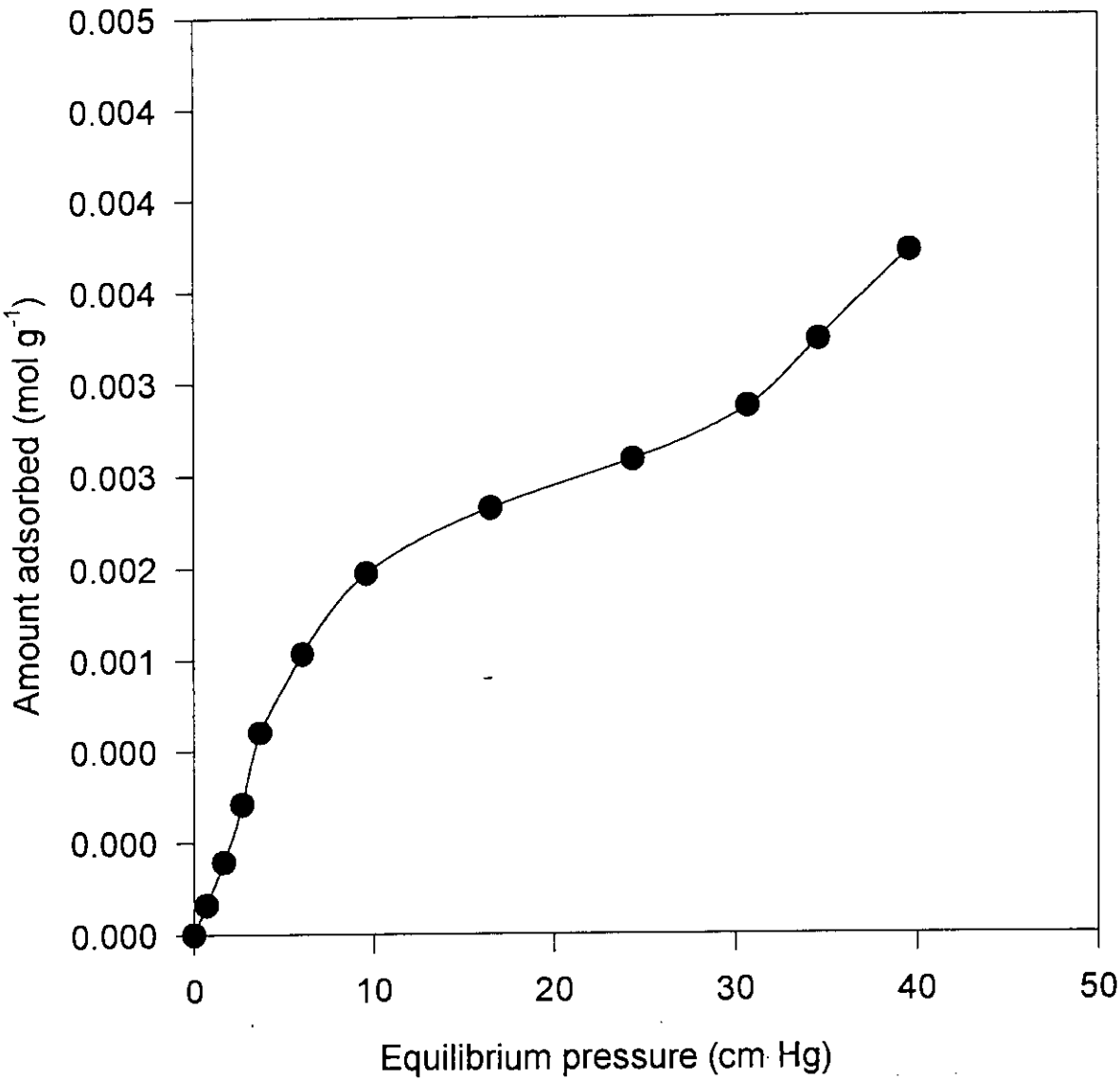

Fig-3.4.11: Isotherm for adsorption of N_2 at 75K on PAN/silica prepared at pH 11.3 and temperature 27^0C

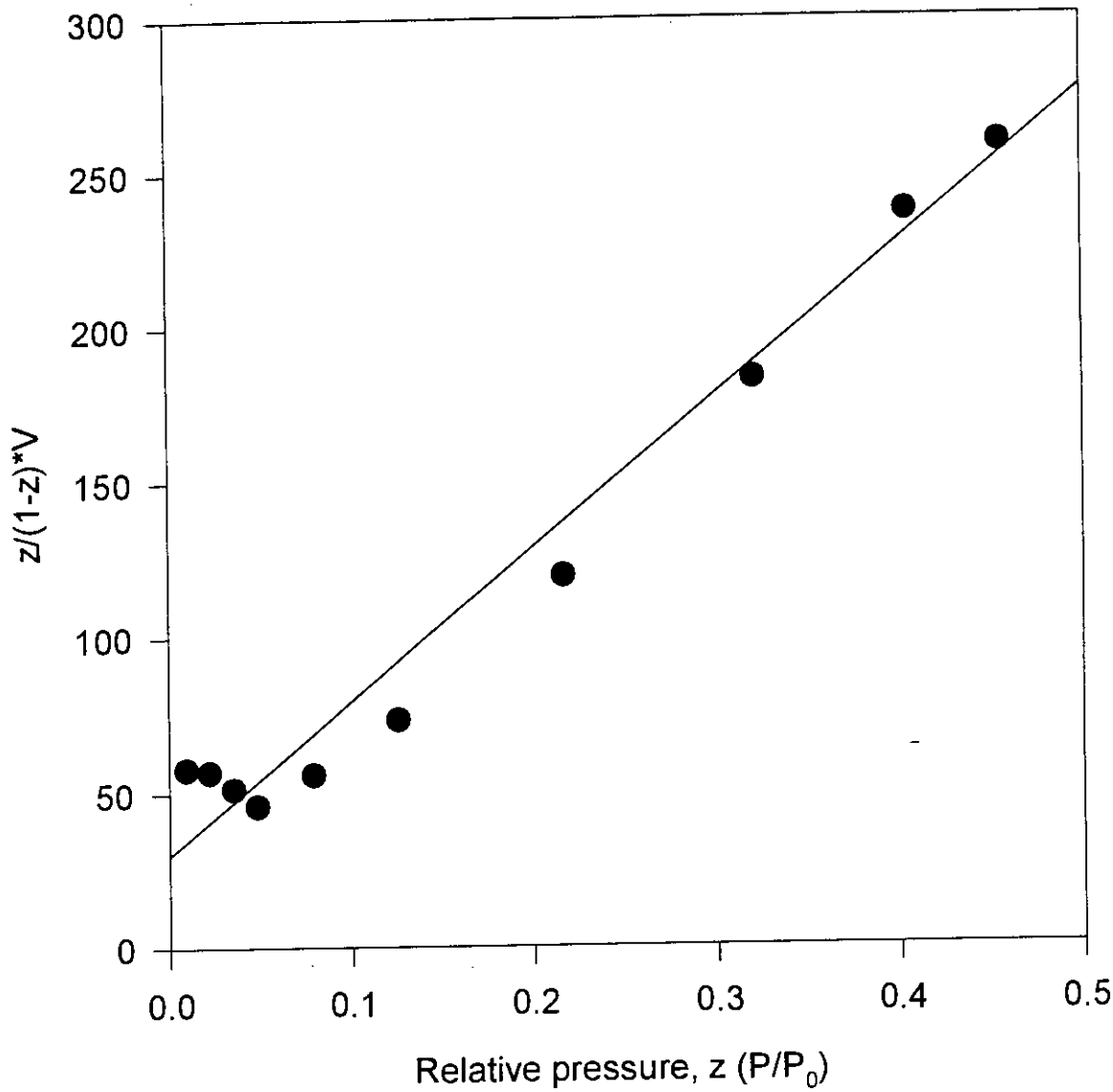

Fig-3.4.12: Linear plot of z/(1-z)*V vs z, where $z = P/P_0$, according to BET equation for PAN/silica prepared at pH 11.3 and temperature 27^0C

3.4.3. BET investigation with CH_3-PAN/silica and Cl-PAN/silica

CH_3-PAN/silica and Cl-PAN/silica composites were prepared at pH 7 and 27^0C. Adsorption of nitrogen for BET surface area measurements were also carried out as the procedure described for PAN/silica samples. The adsorption data are presented in Tables- 3.4.7 and 3.4.8. Figs. 3.4.13 and 3.4.15 show the isotherms. The measurements were carried up to a relative pressure of about 0.6. Figs. 3.4.14 and 3.4.16 show the linear BET plots. The surface area of the composites were evaluated and found to be 53.3 and 68.4 m^2g^{-1} for CH_3-PAN/silica and Cl-PAN/silica respectively. The values are higher than that of the bulk PAN but smaller than those of PAN/silica composites. This results may indicate the influence of functional group on the particle size and porosity of the synthesized materials. The bulkiness or the electronic nature of the $-CH_3$ and –Cl groups may play a role in reducing the surface area and/or porosity of the CH_3-PAN/silica and Cl-PAN/silica composites. However, at present the lower surface area of these two matrices can not be justified properly it would need further investigations.

Table-3.4.7 : Data for the adsorption of N_2 at 75K on CH_3-PAN/silica znanocomposites prepared at pH 7 and temperature 27^0C

Experiment number	Equilibrium pressure (cm-Hg)	Relative pressure (P/P_0)	Amount adsorbed (mol g^{-1})x10^3	Surface area (m^2/g)
1	0.0000	0.0000	0.0000	53.3
2	3.0100	0.0396	0.9068	
3	9.0150	0.1186	1.1052	
4	15.640	0.2058	1.1460	
5	19.450	0.2559	1.1681	
6	25.180	0.3313	1.2075	
7	29.090	0.3828	1.2352	
8	33.580	0.4418	1.2399	
9	38.190	0.5025	1.2701	
10	43.035	0.5662	1.2874	
11	47.360	0.6232	1.3456	
12	50.600	0.6658	1.3925	
13	53.105	0.6987	1.5921	

Table-3.4.8 : Data for the adsorption of N_2 at 75K on Cl-PAN/silica nanocomposites prepared at pH 7 and temperature 27^0C

Experiment number	Equilibrium pressure (cm-Hg)	Relative pressure (P/P_0)	Amount adsorbed (mol g^{-1})x10^3	Surface area (m^2/g)
1	0.0000	0.0000	0.0000	68.4
2	0.1200	1.5789e-3	0.1063	
3	0.6200	8.1579e-3	0.3046	
4	1.6650	0.0219	0.5271	
5	3.6650	0.0482	0.7994	
6	8.1150	0.1068	1.0486	
7	14.1350	0.1860	1.2421	
8	21.0100	0.2764	1.3826	
9	28.9950	0.3815	1.4579	
10	35.4550	0.4665	1.5057	
11	42.2650	0.5561	1.5312	
12	46.1250	0.6069	1.6793	
13	50.2350	0.6610	1.882C	

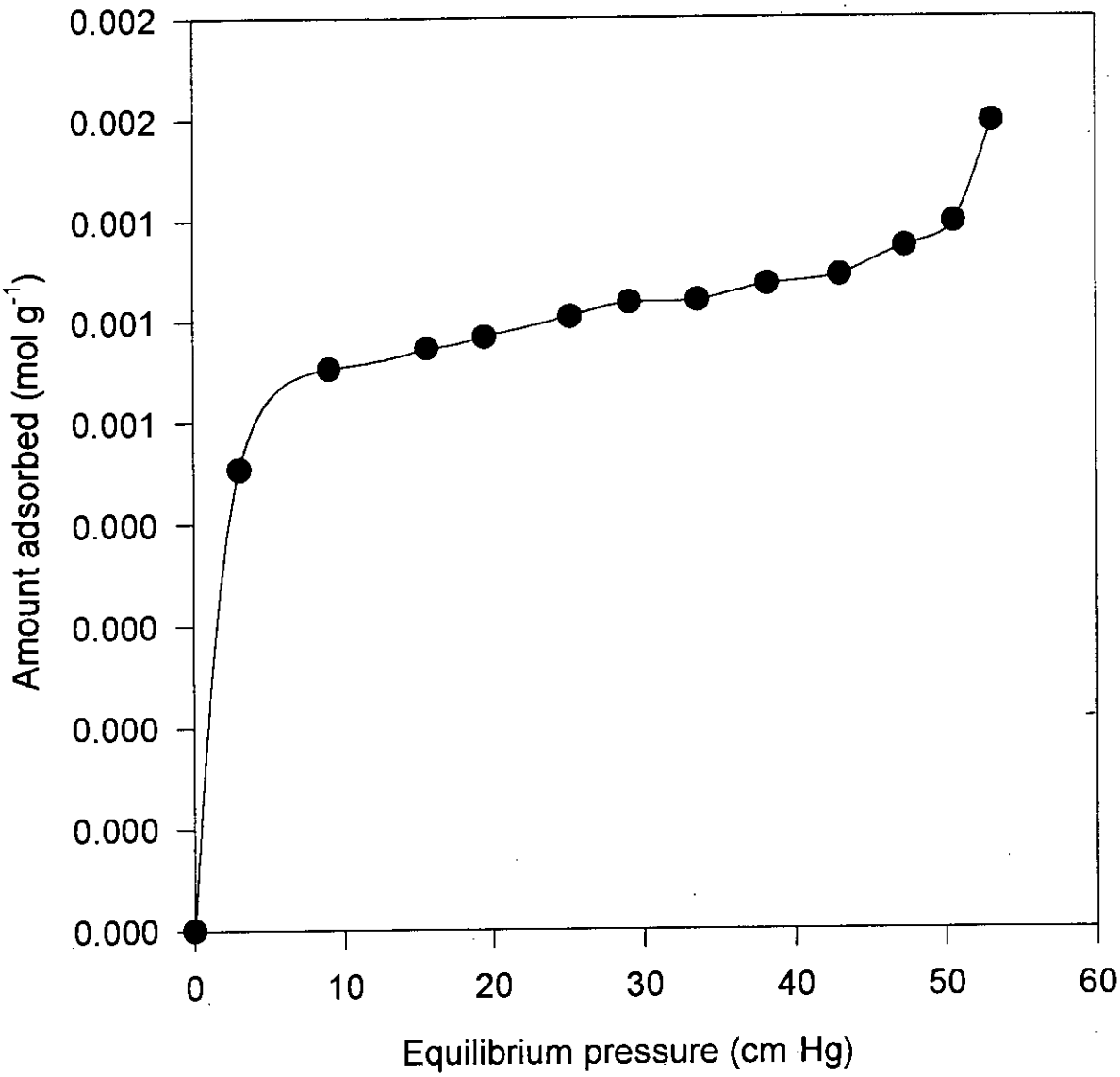

Fig-3.4.13: Isotherm for adsorption of N_2 at 75K on CH_3-PAN/silica prepared at pH 7 and temperature 27^0C.

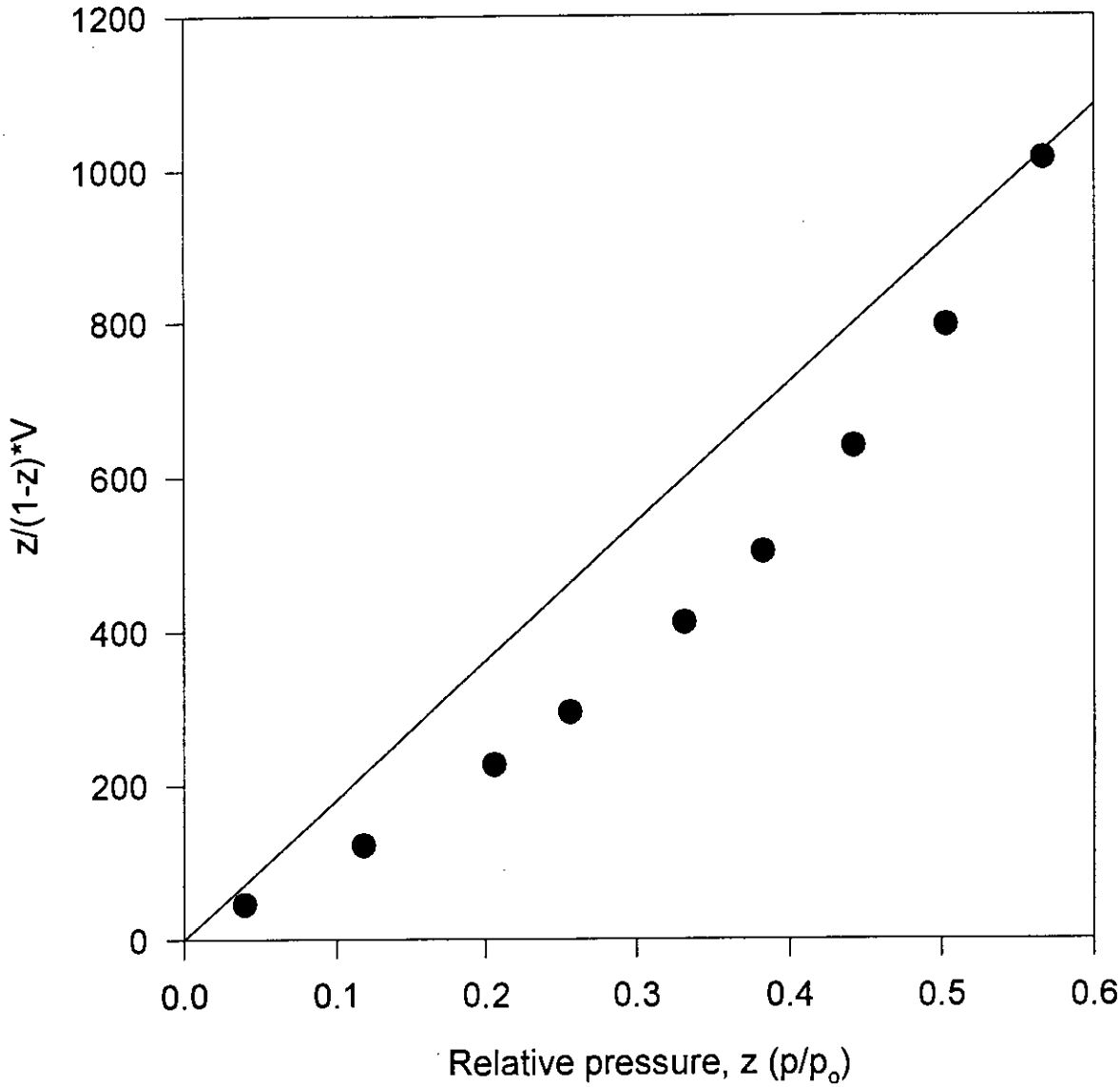

Fig-3.4.14: Linear plot of z/(1-z)*V vs z, where z = P/P_0, according to BET equation for CH_3-PAN/silica prepared at pH 7 and temperature 27^0C

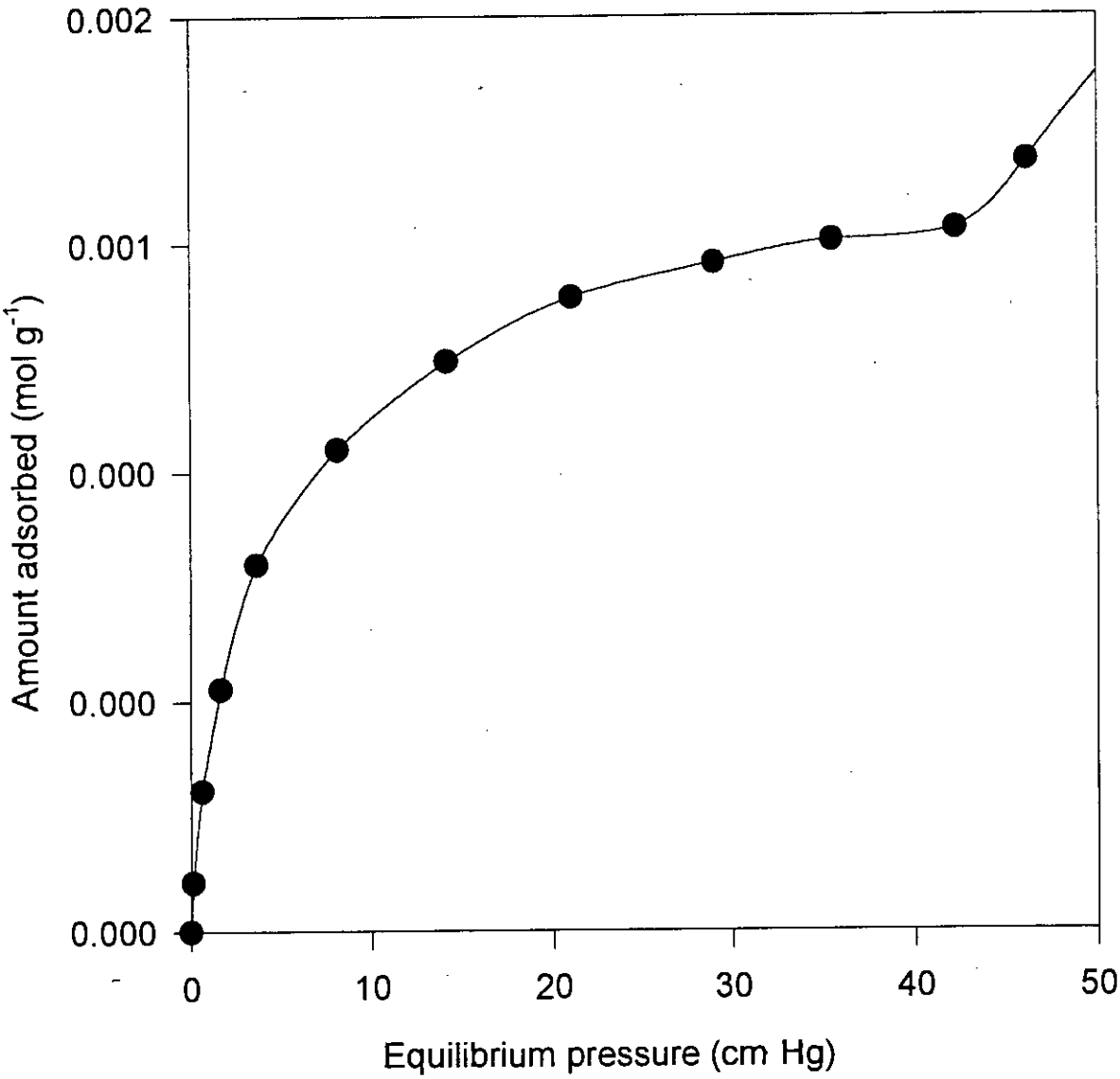

Fig-3.4.15: Isotherm for adsorption of N_2 at 75K on Cl-PAN/silica prepared at pH 7 and temperature 27^0C

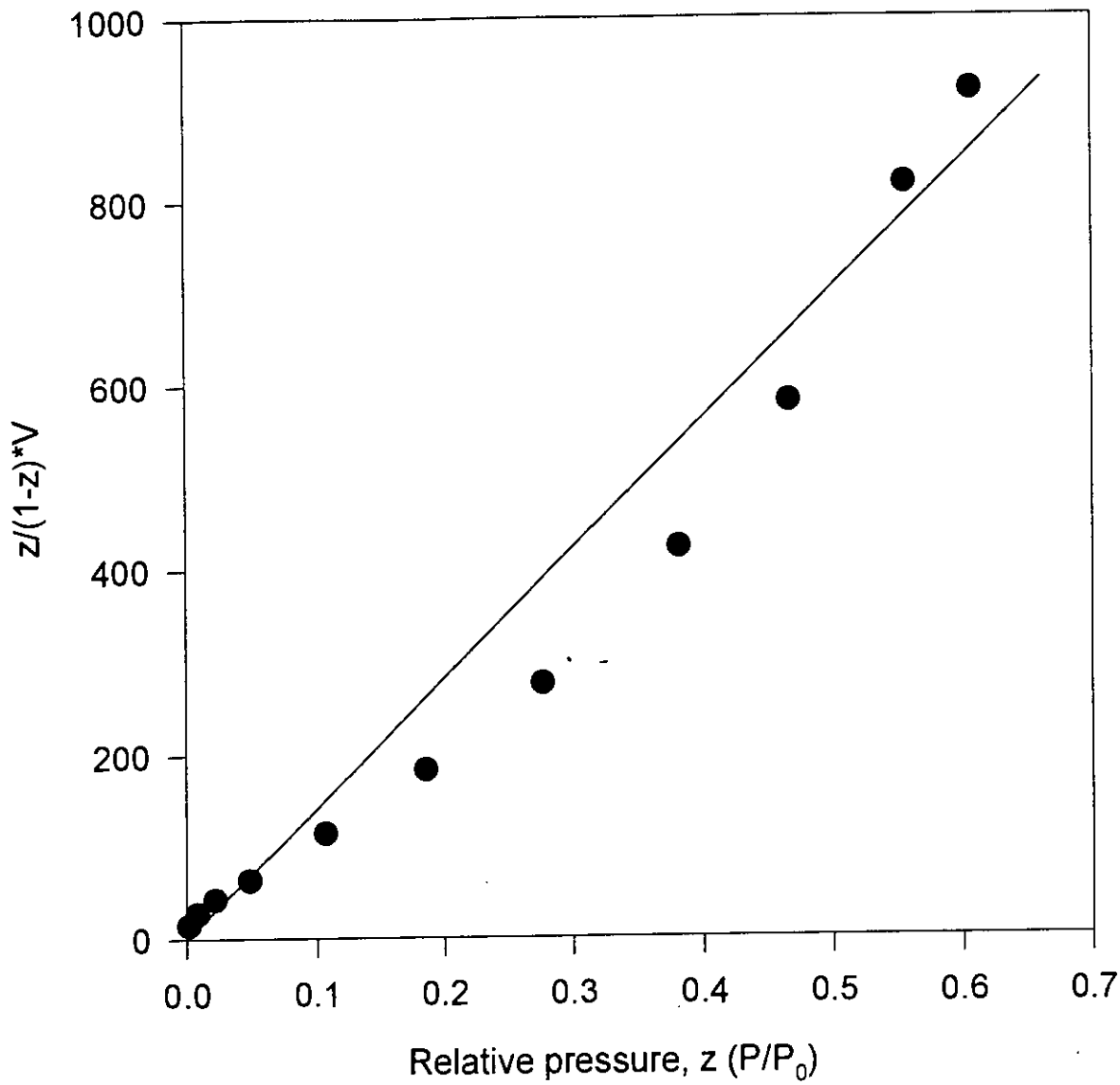

Fig-3.4.16: Linear plot of z/(1-z)*V vs z, where $z = P/P_0$, according to BET equation for Cl-PAN/silica prepared at pH 7 and temperature 27^0C

Table- 3.4.9. Data for the BET surface area of the studied samples.

Name of the sample	Preparation condition		Surface area (m^2/g)
	pH	Temp.(^0C)	
PAN	7	27	25.9
PAN/silica	7	0	160.2
PAN/silica	7	27	252.7
PAN/silica	7	50	184.3
PAN/silica	3.1	27	127.3
PAN/silica	11.3	27	178.4
CH_3-PAN/silica	7	27	53.3
Cl-PAN/silica	7	27	68.4

References

1. Bjorklund, R. B., and Liedberg, B., *J. Chem. Soc. Chem. Commun,* 1293 (1986).
2. Armes, S. P., and Aldissi, M., *Polymer*, **31**, 569, 1990.
3. Epron, F., Henrg, F., and Sagnes, O., *Makromol. Chem., Macromol.,* **35/36**, 527, (1990).
4. Olegard, R., Skotheim, T. A., and Lee, H.S., *J. Electrochem. Soc.* **138,** 2930, (1991).
5. Armes, S. P., Aldissi, M., Agnew, S. F., and Gottesfeld, S., *Langmuir,* **6,** 1745 (1990).
6. Gill, M., Mykytiuk, J., Armes, S.P., Edward, J. L., Yeates, T., Moreland, P. J, and Mollett, C., *J. Chem. Commun*, 108 (1992).
7. Gill, M., Armes, S. P., Fairhurst, D., Emmett, S. N, Idzorok, G., and Pigott, T., *Langmuir,* **8**, 2178 (1992).
8. Gill, M., Baines, F. L., and Armes, S. P., *Synth Met,* **55-57**, 1029, (1993).
9. Bocchi, V., Chierici, L., and Gardini, G. P, *Tetrahedron*, **26**, 4073, (1970).
10. Machida, S., Miyata, S., and Techagumpuch, A., *Synth. Met.*, **31**, (1989).
11. Terrill, N. J., Crowley, T., Gill, M., and Armes, S. P., *Langmuir*, **9**, 2093, (1993).
12. Hung, W. S., Humphrey, B. D., and MacDiarmid, A. G., *J. Chem. Soc., Faraday, Trans.*, **1**, 2385, (1986).
13. Stejskal, J., Kratochvil, P., and Jenkins, A. D., *Polymer*, **37**, 367, (1996).

14. Stejskal, J., Kratochvil, P., Armes, S. P., Lascelles, S. F., Riede, A., Helmstedt, M., Prokes, J., and Krivka, I., *Macromoleculs*, **29**, 6814, (1996).

15. Maeda, S., and Armes, S. P., *Synth. Met.*, **73**, 151, (1995).

16. Maeda, S., and Armes, S. P., *J. Mater, Chem.*, **4(6)**, 935, (1994).

17. Maeda, S., Gill, M., Armes, S. P., and Fletcher, I. W., *Langmuir*, **11**, 1899, (1995).

18. Butterworth, M. D., Maeda, S., Johal, J., Corradi, R., Lascelles, S. F., and Armes, S. P., *J. Colloid Interface Sci.*, **174**, 510, (1995).

19. Sharma, Y. R., Elementary Organic Spectroscopy, S. Chand Company Ltd., New Delhi, India, P- 80, (1993).

20. Pavia, D. L., Lampman, G. M., Kriz, G. S., Introduction to spectroscopy, Saunder College Publishing, USA, P- 26, 38, 63, (1979).

21. Dyer, J. R., Application of Absorption Spectroscopy of Organic Compounds, Prentice-Hall of India Private Ltd., New Delhi, India, P- 37, (1991).

22. Nakamoto, K., Infra-red and Raman Spectra of Inorganic and Co-Ordination Compounds, John Willey and Sons, New York, USA, P- 242, (1983).

23. De Surville, R., Doriomedoff, M., Cristofini, F. H., Josefowicz, M., Yu, L. T., and Buvet, R., *J. Chem. Phys.*, **68**, 1055, (1971).

24. Ginder, J. M., and Epstein, A. *J., Phys. Rev.*, **B41**, 10674, (1990).

25. Perruchot, C., Chehimi, M. M., Delamar, M., Lascelles, S. F., and Armes, S. P., *J. Colloid Interface Sci.*, **193**, 190 (1997).

26. M. Muhibur Rahman, Department of Chemistry, University of Dhaka, Personal communication.

27. Meyer E. F., *J. Chem. Ed.* **57,** 120 (1980)

28. Dorris, G. M., and Grey, D. G., *J. Colloid Interface Sci.* 77, 353 (1980)

29. Chehimi, M. M., Abel, M-L. and Sharaoui, Z., *J. Adhesion Sci. Technol.* **10,** 287 (1996).

Chapter 4
Conclusion

Conclusion

The polymerization of aniline, *o*-toluidine and 2-chloroaniline in the presence of sodium silicate solution represents a novel and facile route for the preparation of organic polymer-silica colloidal dispersion which utilizes commercially available sodium silicate particles as dispersants. These polymer/silica composites represent a potentially useful processible form of poly(aniline) and its derivatives, normally intractable conducting polymer. These dispersions have good long term colloidal stability. Colloids of the prepared nanocomposites have been found stable at different pH and temperature of the synthesis medium. Derivatives of aniline with electron releasing and withdrawing groups when used in the composites synthesized also produces good colloidal stability as high as poly(aniline)/silica samples. Optical microscopic studies confirm that the polymer/silica composites are made up of microaggregates of the original small silica particles. Densities of the polymer-silica becomes significantly higher than that of the corresponding bulk polymers. Weight-average particle size distribution of the studied composites indicates a wide distribution of the particles. Even by changing the synthesize conditions e.g. pH and temperature, these particles distribution have been found unchanged i.e. the distribution remains broad. Therefore, optimization of the synthesize condition is required to have a reasonably narrow particle-size distribution and may therefore be of interest as "model colloids".

The nanocomposites were characterized by inverse gas chromatography and indicated that the studied nanocomposites behave as high surface energy materials as judge by the dispersive contributions to their surface free energies

(γ_s^d). These γ_s^d values exceed that of the reference bulk powder PAN. IGC experiment also indicated that the synthesized composites have separative capacity to separate alkanes (C_5-C_9) from their mixture and therefore can be used as model column materials.

The prepared nanocomposite particles which have been synthesized utilizing commercially available sodium silicate solution, have more than four times higher BET surface areas than that of the nanocomposites prepared from colloidal silica dispersion. The observed surface areas of the present samples are nearly ten times higher than that of the corresponding conducting polymer bulk powders. Although silica contents of the composites prepared at different pH and temperature, have been found to be the same, the experimentally observed BET surface area for these samples are different. These findings may suggest that synthesis condition e.g. pH and temperature may have influence on the porosity or the particle size of the synthesized materials to exhibit the different surface area of the samples having the almost same amount of silica. When derivatives of aniline with electron releasing and withdrawing groups were used in the preparation of polymer-silica composites BET measurements predicted a significantly lower surface area than that of PAN/silica matrix. These derivatives materials seems to be interesting for further investigation since they possess different electronic atmosphere which might play an important role in the preparation of new materials substrates.

Appendix

Appendix

Primary data for the adsorption isotherm

Sample-PAN/silica (prepared at pH 7 and at 27^0C)

Weight of the sample: 1.436 g

Room temperature: 304.86 K

Temperature of the experiment: 75 K

Volume of the adsorption vessel: 33.08 cm^3

Reference scale reading: 78.5 cm

Dose-1	**(cm)**
Initial scale reading	72.550
First scale reading	75.800
Equilibrium scale reading	78.160
Dose-2	
Initial scale reading	69.390
First scale reading	75.600
Equilibrium scale reading	78.550
Dose-3	
Initial scale reading	64.535
First scale reading	65.225
Equilibrium scale reading	68.100

Dose-4	
Initial scale reading	59.680
First scale reading	71.455
Equilibrium scale reading	76.365
Dose-5	
Initial scale reading	54.770
First scale reading	67.280
Equilibrium scale reading	72.240
Dose-6	
Initial scale reading	53.290
First scale reading	63.145
Equilibrium scale reading	66.915
Dose-7	
Initial scale reading	49.365
First scale reading	57.855
Equilibrium scale reading	60.975
Dose-8	
Initial scale reading	44.360
First scale reading	52.315
Equilibrium scale reading	55.940

Dose-9	
Initial scale reading	39.980
First scale reading	47.685
Equilibrium scale reading	51.425
Dose-10	
Initial scale reading	34.040
First scale reading	42.565
Equilibrium scale reading	46.780
Dose-11	
Initial scale reading	24.080
First scale reading	35.180
Equilibrium scale reading	41.745
Dose-12	
Initial scale reading	15.005
First scale reading	21.185
Equilibrium scale reading	32.820
Dose-13	
Initial scale reading	13.095
First scale reading	18.550
Equilibrium scale reading	29.335

List of the symbols and abbreviations

Symbols/Abbreviations	Explanation
PP	Poly(pyrrole)
PAN	Poly(aniline)
PAN/silica	Poly(aniline)/silica
CH_3-PAN/silica	Poly(*o*-toluidine)/silica
Cl-PAN/silica	Poly(2-chloroaniline)/silica
IR	Infra-red
IGC	Inverse gas chromatography